Int J Earth Sci (Geol Rundsch) (2004) 93:361–383
DOI 10.1007/s00531-004-0386-7

ORIGINAL PAPER

U. A. Glasmacher · I. Matenaar · W. Bauer · V. N. Puchkov

Diagenesis and incipient metamorphism in the western fold-and-thrust belt, SW Urals, Russia

Received: 2 October 2002 / Accepted: 17 January 2004 / Published online: 1 May 2004

Abstract In the western fold-and-thrust belt of the southern Urals, the Kübler and Árkai indices determined on shales, slates and phyllites record an increase from lower late diagenetic to epizonal grade from west to east. The metamorphic grade varies strongly within the different tectonic segments, which are separated by major thrusts. The increase of diagenetic and incipient metamorphic grade from the footwall to the hanging wall of all major Upper Palaeozoic thrusts indicates a pre-Permo/Triassic origin. West of the Avzyan thrust zone, the diagenetic to incipient metamorphic grade is related to the Palaeozoic basin development and reached the final grades in Late Carboniferous to Early Permian times. East of the first Avzyan thrust in the Yamantau anticlinorium, the diagenetic to lower greenschist metamorphic grade is possibly of Neoproterozoic origin and might be related to the development of the Neoproterozoic basin at the eastern margin of the East European Craton. The eastern part of the Yamantau anticlinorium was exhumed below 200 °C in the Late Carboniferous or Early Permian. The diagenetic grade of the autochthonous Palaeozoic sedimentary units increases toward the stack of Palaeozoic nappes and might partly be caused by the deformational process due to the emplacement of the Palaeozoic nappes. Within the Timirovo thrust sheet, the decrease of metamorphic grade with stratigraphic age developed prior to the emplacement of the nappes. The upper anchizonal metamorphic grade of the Upper Devonian slates of the Zilair nappe results from the deformation process related to the Lower Carboniferous nappe emplacement.

Keywords Diagenesis · Incipient metamorphism · Kübler and Árkai indices · Southern Urals · URSEIS'95

U. A. Glasmacher (✉)
Forschungsstelle Archäometrie der Heidelberger Akademie der Wissenschaften,
Max-Planck-Institut für Kernphysik,
Postfach 103980, Heidelberg, Germany
e-mail: ua.glasmacher@mpi-hd.mpg.de
Tel.: +49-6221-516321
Fax: +49-6221-516633

I. Matenaar · W. Bauer
Geologisches Institut, RWTH Aachen,
Wüllnerstrasse 2, 52056 Aachen, Germany

V. N. Puchkov
Ufimian Geoscience Center,
Russian Academy of Sciences,
K. Marx Str., 450000 Ufa, Russia

Introduction

The Uralide orogen forms a linear N–S-trending Palaeozoic fold-and-thrust belt that extends for more than 2,000 km from the Arctic Ocean to near the Caspian Sea (Fig. 1). It resulted from the Palaeozoic two-stage collision of the East European Craton (EEC) with the Sibirian/Kazakhstanian continents and intervening accretion of island arc and microcontinental fragments (Hamilton 1970; Zonenshain et al. 1984, 1990; Puchkov 1988, 1993, 1997). The Main Uralian fault (MUF) is the major suture zone between the East European Craton to the west and the oceanic, island arc and continental terranes of Asia to the east (Zonenshain et al. 1984, 1990; Echtler and Hetzel 1997). In comparison to other Palaeozoic orogens (e.g. the Variscides, Caledonides etc.), the Uralides show a general bilateral symmetry with a western fold-and-thrust belt, a central magmatic arc zone (Magnitogorsk zone) and an eastern thrust belt with deep reaching crustal shear zones (Berzin et al. 1996). However, unlike other Palaeozoic orogens that underwent post-orogenic collapse and extension, the Uralide fold belt reveals an intact, well-preserved orogen with a deep crustal root within a stable continental interior (Echtler et al. 1996; Steer et al. 1998). The crustal root is interpreted as partially eclogitized lower crust (Döring and Götze 1999; Leech 2001). As the orogen is isostatically compensated and appears as though it has never departed far from this state, it represents an orogen that has escaped delamination of the lower crust and post-orogenic extensional collapse (Giese 2000; Leech 2001). Thus, the Uralides are an exceptional ex-

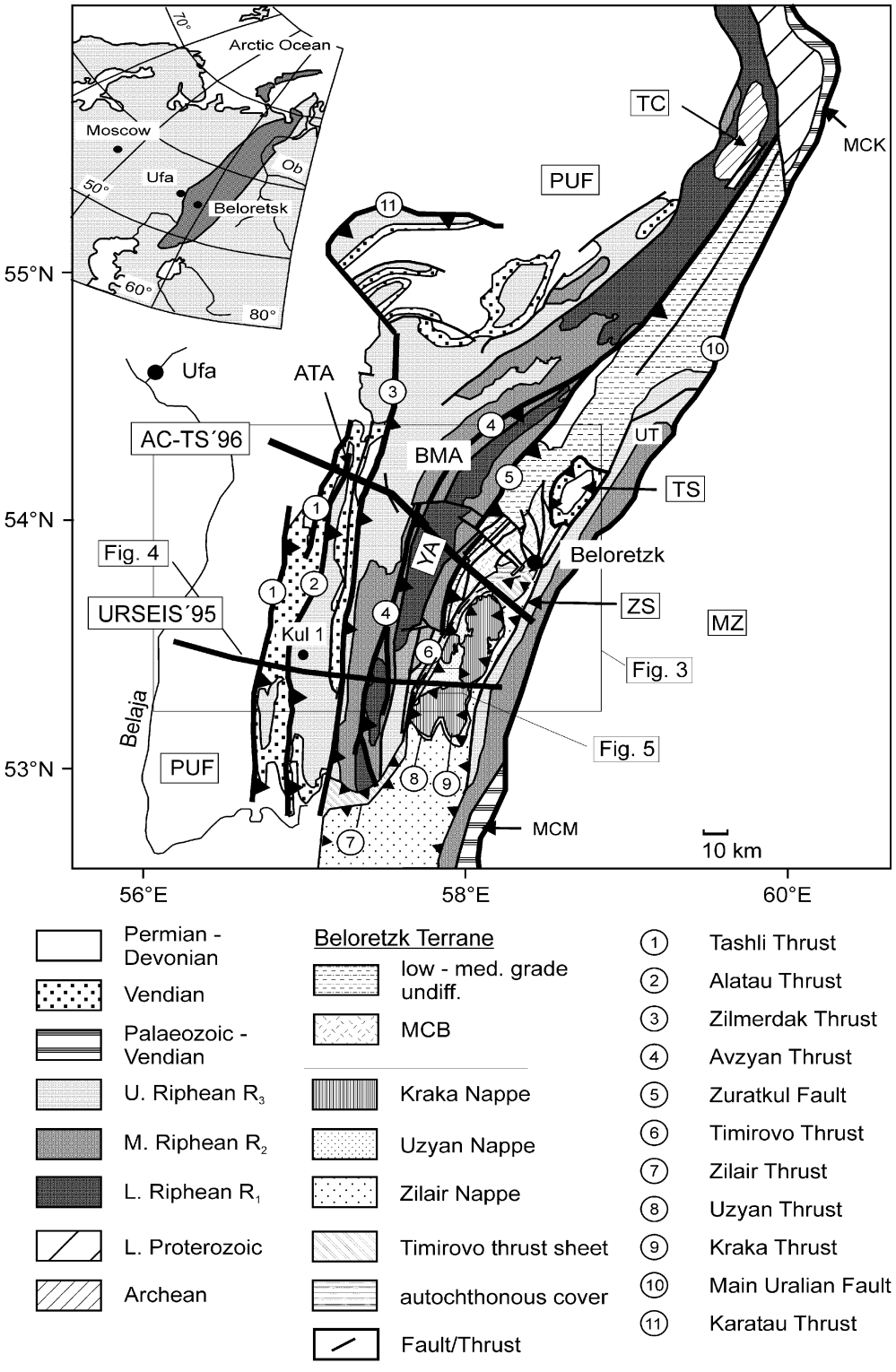

Fig. 1 Geological map of the western part of the southern Uralides (based on 1:200,000 scale geological map. *ATA* Ala-Tau anticlinorium; *BMA* Bashkirian Mega-anticlinorium; *MCB* metamorphic complex of Beloretzk; *MCK* metamorphic complex of Kurtinsky; *MCM* metamorphic complex of Maksyutov; *PUF* pre-Uralian foredeep; *TC* Taratash complex; *TS* Tirlyan synclinorium; *UT* Ural-Tau; *YA* Yamantau anticlinorium; *ZS* Zilair synclinorium; *MZ* Magnitogorsk zone

ample that allows the study of the pre-, syn- and post-orogenic tectono-thermal evolution of a Palaeozoic orogen.

The diagenetic to incipient metamorphic grade of Palaeozoic and Precambrian shales, slates and phyllites was studied in detail along the 120-km-long western part of the W-E URSEIS'95 transect in the western fold-and-thrust belt of the southern Urals, Russia. The western part of this transect extends from the Devonian to Permian sedimentary units of the Pre-Uralian foredeep, crossing the Precambrian siliciclastic and carbonate units of the Bashkirian Mega-anticlinorium, to the Palaeozoic units of the Ural-Tau antiform.

The present study combines Kübler and Árkai indices of shales, slates and phyllites to quantify the finite meta-

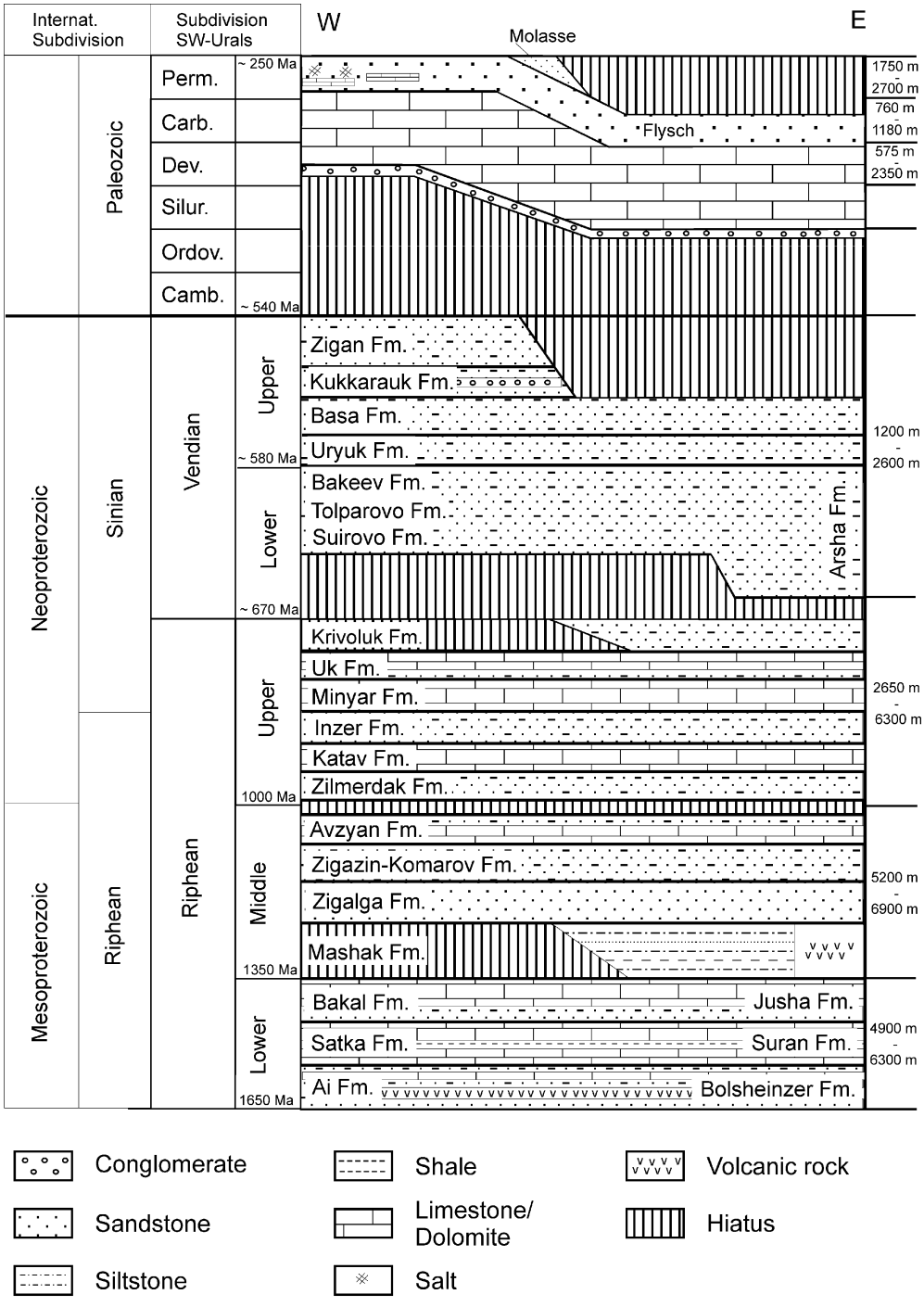

Fig. 2 Stratigraphic subdivision of the western fold-and-thrust belt, SW Uralides (according to Kozlov et al. 1995; Maslov et al. 1997, international time-scale after Haq and Eysinga 1998) vertical hatching: hiatus; *v*: volcanic rocks

morphic grade along the W–E-trending URSEIS'95 transect and the Kulgunina drill hole (Kul 1), which is located 5 km north of the URSEIS'95 transect (Fig. 1). The finite metamorphic grades along the URSEIS'95 transect will be compared with finite metamorphic grade data acquired along the W–E-trending AC-TS'96 transect 80 km to the north (Glasmacher et al. 1997; Matenaar et al. 1999). Consideration of apatite and zircon fission-track data of sandstones, quartzites and dikes (Seward et al. 1997; Glasmacher et al. 2002) will further constraint the thermal history.

Regional geology

The most prominent feature of the western part of the southern Uralides is the Bashkirian Mega-anticlinorium (BMA), a broad NE- and SSW-plunging antiformal structure composed of over 10,000-m-thick Precambrian sedimentary strata (Figs. 1, 2 and 3; Kozlov 1982). Meso- to Neoproterozoic siliciclastic and carbonate units of the BMA are formed in terrestrial fluvial to shallow marine environment (Fig. 2; Kozlov et al. 1989, 1995; Maslov et al. 1997). The thickness of the Zilmerdak Formation

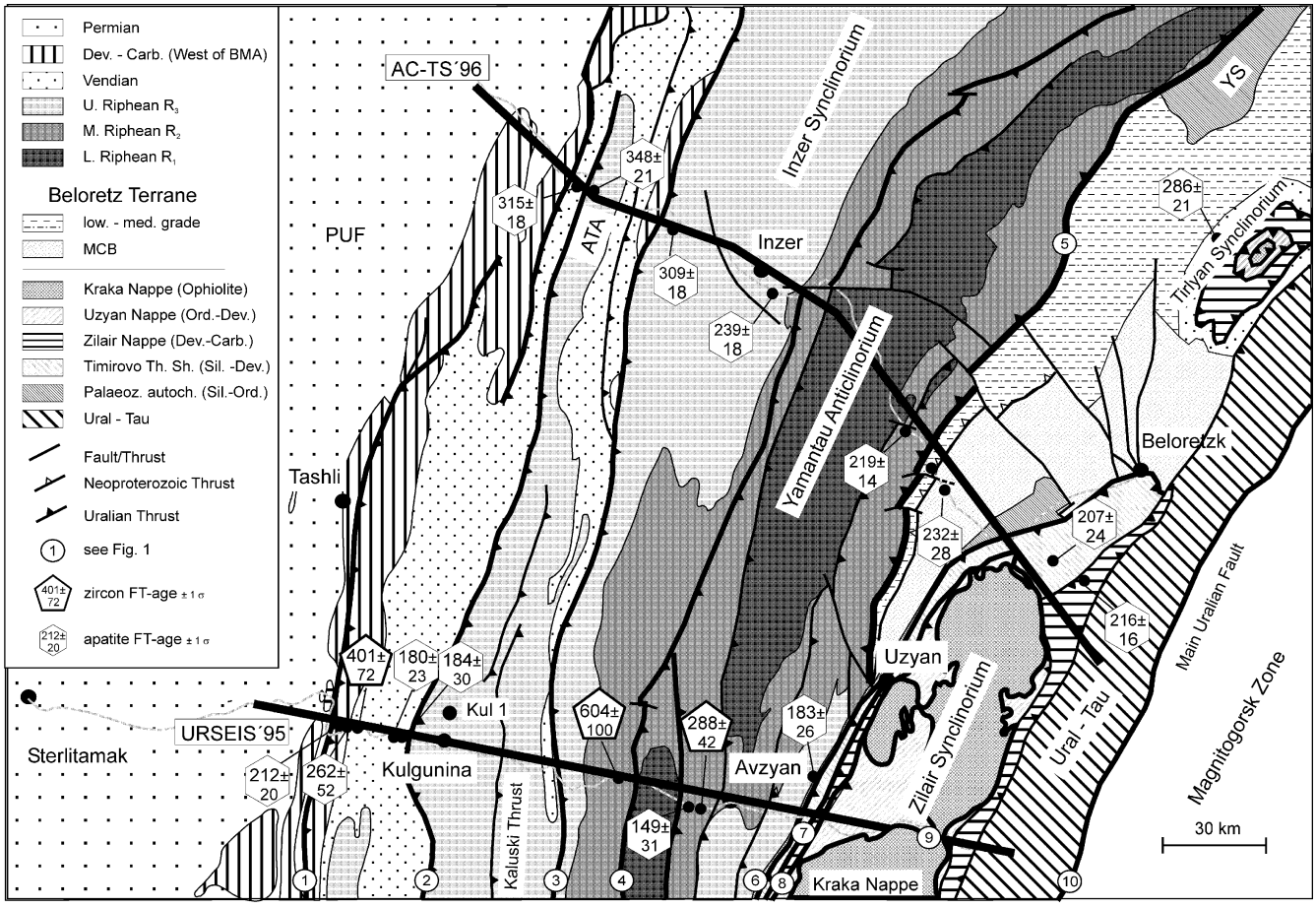

Fig. 3 Geological map of the investigated area (based on 1:200,000 scale geological map, Giese et al. 1999). Fission-track data after Seward et al. (1997)

(lowermost Upper Riphean) varies strongly between ~600 m and >3,000 m, respectively, West and East of the Zilmerdak thrust. Upper Vendian polymict siliciclastic units are interpreted as flysch and molasse deposits of a Neoproterozoic orogenic event at the eastern margin of Baltica (Puchkov 1997; Stroink et al. 1997; Giese et al. 1999; Glasmacher et al. 2001; Willner et al. 2001). In the west, the Tashli thrust separates the gently deformed Devonian to Permian strata (3,000 m thickness) of the Pre-Uralian Foredeep (PUF) from the folded structures of the BMA (Fig. 1). During the Permian, the PUF formed the western foreland basin of the Uralian orogeny with barrier reef complexes developed synchronously to prograding flysch sedimentation from the east. Early Permian evaporites controlled the deformation and resulted in important ridge-like salt diapirs.

The fold-and-thrust belt of the BMA is characterized by longitudinal regional-scale synclinal and anticlinal structures (from West to East: Ala-Tau anticlinorium, Inzer synclinorium, Yamantau anticlinorium) that are separated by important thrusts (Ala-Tau thrust, Zilmerdak thrust, Avzyan thrust zone). In the north, east and south of the Ala-Tau anticlinorium, Vendian flysch deposits are overlain by Devonian to Carboniferous siliciclastic and carbonate units of about 2,500 m thickness (Puchkov 2000).

The Zuratkul Fault, the most prominent tectonic boundary in the BMA, can be traced south from the eastern limb of the Taratash complex approximately 300 km into the BMA (Fig. 1). It is the site of a major structural and metamorphic break. Based on new structural, metamorphic and chronometric data, Glasmacher et al. (1999, 2001) reinterpreted the Zuratkul fault as a major terrane boundary that separates Neo- and Mesoproterozoic sedimentary units of the EEC from Mesoproterozoic low- to high-grade metamorphic units of the allochthonous Beloretzk Terrane.

East and south of the BMA, the Zilair synclinorium (Fig. 3) forms a SW-plunging, broad synform of Ordovician to Devonian siliciclastic and carbonate sedimentary rocks that unconformably overlie the Beloretzk Terrane (Figs. 1 and 3; Giese et al. 1999; Glasmacher et al. 2001). Tectonically, the Zilair synclinorium consists of a Palaeozoic autochthonous unit at the base, overlain by the Timirovo thrust sheet, and of a stack of nappes (Zilair nappe, Uzyan nappe, Kraka nappe). Close to the unconformity at the AC-TS'96 transect, the Ordovician and Silurian sedimentary rocks are almost undeformed

(Palaeozoic autochthonous). Towards the east and along strike towards the south the deformation increases. The first major thrust of the Timirovo thrust sheet is located at the base of the Devonian limestones. East of this thrust, all rocks show NW-vergent folding and axial-planar cleavage. The late Devonian Zilair flysch, which increases in thickness towards the south forms the entire core of the synclinorium and is comprised of, according to Brown et al. (1996, 1998), Bastida et al. (1997) and Puchkov (1997), the Zilair nappe (Fig. 3). The Zilair nappe is overthrusted by the Uzyan nappe, an imbricated unit of Ordovician to Devonian continental rise sedimentary rocks. Separated by a basal melange, the Kraka ophiolite complex, a nappe of unknown age, overlies the Uzyan nappe.

Geodynamic evolution

The Palaeozoic shelf platform of the East European Craton (EEC) is underlain by an outboard high-level metamorphic block, which consolidated during the Neoproterozoic orogeny (Glasmacher et al. 1999, 2001). Towards the interior of the EEC, Palaeozoic shelf sedimentary rocks overlie a rift basin containing up to 15,000-m-thick sedimentary units of Riphean age (Fig. 2). The onset of Uralian collision-related deformation is generally accepted to have taken place during Middle to Late Devonian times (Brown et al. 1997, 2000; Brown and Spadea 1999). This is based on radiometric ages of about 385–365 Ma for the HP metamorphism in the Maksyutovo complex, and the onset of the Zilair flysch sedimentation at the beginning of the Famennian, i.e. 370 Ma ago (Matte et al. 1993; Shatsky et al. 1997; Hetzel et al. 1998; Brown et al. 1998, 2000, 2001; Beane and Connelly 2000; Remaine et al. 2000, Glodny et al. 2002). Tectonic accretion of oceanic crust and basin-and-slope units resulted in an accretion complex, which prograded towards the NW and moved onto the EEC. Continuous NW–SE-directed convergence and continental subduction resulted in the formation of an early tectonic wedge at about 340 Ma. The Neoproterozoic metamorphic basement block moved onto the EEC to exhume the accretionary complex. The Zilair synclinorium and the Yamantau anticlinorium are formed as hanging-wall structures when the basal detachment cut into the former Meso- to Neoproterozoic basin. The main shortening of the Uralian deformation occurred during these first two stages in the Middle to Upper Devonian and Lower Carboniferous. The orogenic evolution in the SW Uralides ended in the Late Permian to Lower Triassic with a final phase of E–W-directed shortening. The orogenic wedge propagated further to the west creating the western fold-and-thrust belt, partly by reactivation and inversion of Meso- to Neoproterozoic normal faults (Brown et al. 1999; Giese 2000). Tectonic transport of the hanging wall was directed towards the west. The reconstruction from balanced sections indicates 15 to 20% of tectonic shortening for the tectonic wedge, whereas 8 to 10% of tectonic shortening was estimated for the Pre-Uralian Foredeep (Giese 2000).

Sample description and analytical methods

The Palaeozoic and Precambrian strata were sampled in a spacing of about 2 km along the 120-km-long western part of the W-E URSEIS'95 transect (Figs. 4 and 5, Table 1). Furthermore, 11 samples were taken from the Precambrian strata of the Kulgunino 1 drill core (5,142 m, Fig. 6). The Kulgunino 1 drill side is located at 5 km north of the village Kulgunino and is crossed by the URSEIS'95 seismic experiment (Figs. 3 and 4).

The sample preparation implemented the recommendations of the Working Group on Illite Crystallinity (Kisch 1991). The use of the Kübler index (CIS-$FWHM_{ill001ad}$) for illite crystallinity and the Árkai index (CIS-$FWHM_{Chl002ad)}$ for chlorite crystallinity is in accordance with the recommendations of the AIPEA Nomenclature committee (Guggenheim et al. 2002). The 71 samples were cleaned, broken by hammer and grained with a rotary disk mill for 5 s. Short milling duration was applied to avoid any shear and thermal influence on the <2-µm-size fraction by the milling process (for further discussions see Kisch 1991; Krumm and Buggisch 1991). The milled material was sieved at a 63-µm size and the oversized rock ships milled again. This grinding procedure was repeated until 100–200 g of size fraction <63 µm was obtained. The milling procedure is in agreement with the recommendations of the IGCP 294 IC working group (Kisch 1991) and research results of Reuter (1985), Krumm and Buggisch (1991), Nierhoff (1994), Tschernoster (1995) and Glasmacher et al. (2001). Separation of the <2-µm-size fraction was prepared in Atterberg settling cylinders and the fractions were centrifuged. No cation saturation was applied to the separated fractions.

The bulk mineralogical composition of the <63- and <2-µm size fractions and the Kübler and Árkai indices of the <2-µm-size fraction were determined by using a Siemens D 500 X-ray diffractometer at 35 kV and 30 mA CuKα radiation. To minimize the background signal and to allow the use of the recommended material thickness of 0.3 mg/cm^2 (Krumm and Buggisch 1991), single silicon crystals were used as mounts. Sedimented glass mounts were made with 1 ml of a homogenized size fraction-distillate water-suspension (147 mg/100 ml equals 0.3 mg/cm^2), and air-dried at room temperature. Each mount was scanned from 3 to 63° 2Θ, at a scan-rate of 0.6° 2Θ/min. After determination of the air-dried crystallinity, the samples were left at a temperature of 60 °C for 4 h in an ethylene glycol-saturated atmosphere, and the crystallinity of illite and chlorite were measured again.

The $FWHM_{Ill001ad}$, $FWHM_{Ill001gly}$, $FWHM_{Chl002ad}$ and $FWHM_{Chl002gly}$ were determined as the median value of nine measurements of the full width at half height maximum [°$\Delta 2\Theta$CuKα] of the 10-Å peak ($Illite_{001}$) and 7-Å peak ($Chlorite_{002}$). The peak heights were analysed by using an ASSEMBLER-program, which was programmed

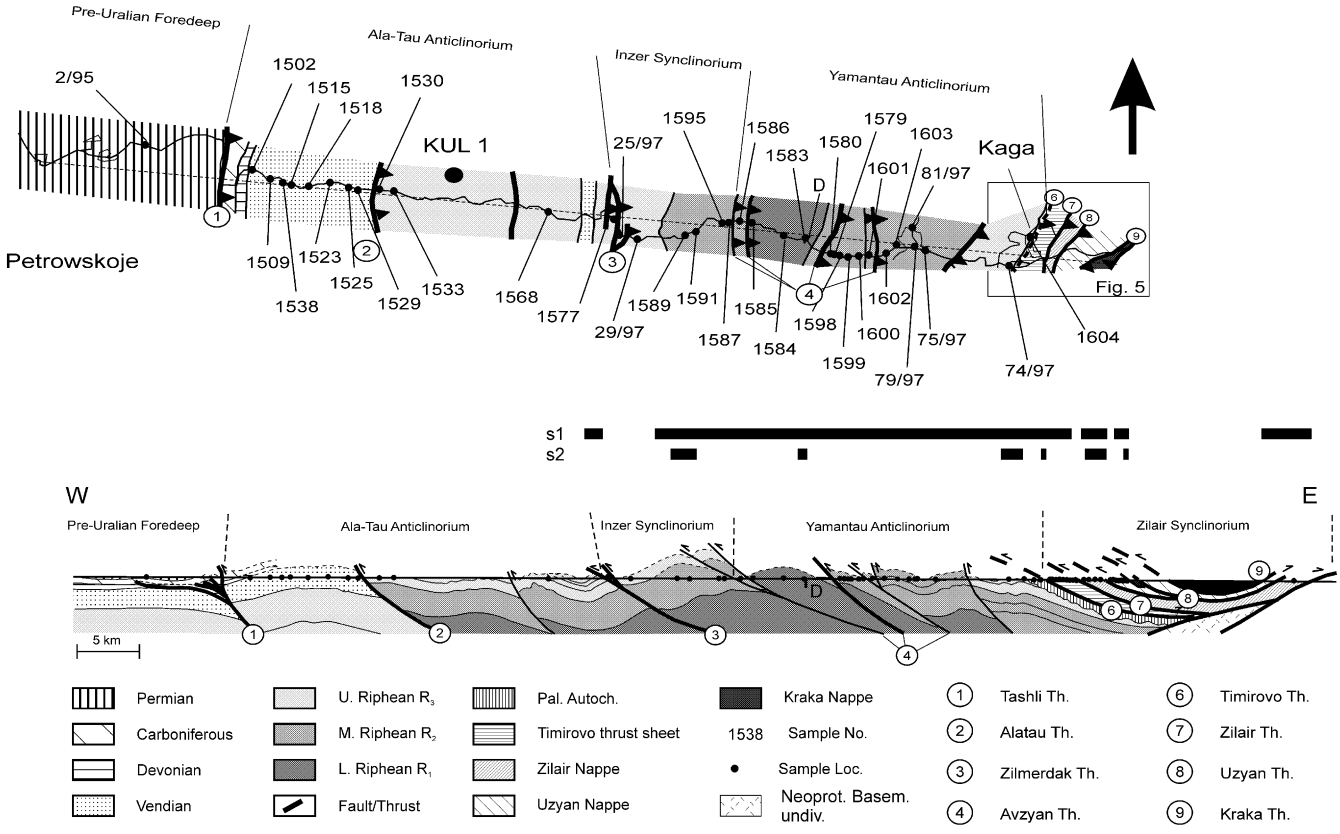

Fig. 4 Detailed geological map (based on 1:50,000 scale geological maps) and generalised WNW–ESE structural cross section (Giese et al. 1999) of the area where the samples were collected (URSEIS'95 transect). Also shown are the sample locations, sample numbers and cleavages. *s1* first cleavage; *s2* second cleavage)

for the DACO-MP (Frank 1987). Calibration of the analytical procedure was made using the recommended standard samples (Warr and Rice 1994). Shortly after sample measurement, the standards were measured 45 times. All data were recalculated to CIS-data. The conversion equations are available from the first author. The boundary between diagenesis and anchizone was set at CIS-$FWHM_{Ill001ad}$=0.42 [°$\Delta 2\Theta$CuKα], and that between anchizone and epizone at CIS-$FWHM_{Ill001ad}$= 0.25 [°$\Delta 2\Theta$CuKα] (Warr and Rice 1994). Boundary values of chlorite crystallinity (diagenesis/anchizone: CIS-$FWHM_{Chl002ad}$=0.33 [°$\Delta 2\Theta$CuKα], CIS-$FWHM_{Chl002ad}$= 0.26 [°$\Delta 2\Theta$CuKα]) were used as described by Árkai (1991) and Árkai et al. (1995, 1996).

As indicated by many researchers, the evolution of the texture on the micrometre-scale plays an important role in interpreting the Kübler and Árkai indices (see for further reading Árkai et al. 2002; Jacob et al. 2000; Passchier and Trouw 1996). Change in both parameters is not solely related to temperature, but the degree of internal deformation (e.g. cleavage development) must be considered when the Kübler and Árkai index values are interpreted. Therefore, descriptive determination of the rock texture at microscopic scale was done by applying a Philipps scanning electron microscope (SEM) at the Geologisches Institut (RWTH Aachen), Germany. Rock specimens were broken either perpendicular to sedimentary textures or perpendicular to the cleavage planes. The broken surface was covered with gold and images were taken at various magnifications. The magnification of 1,600 was chosen to display the textures relevant for the interpretation of textures.

Results

Petrography and textures

Sedimentary textures of the Precambrian to Permian fine-grained, olive grey, green, red and black shales, slates and phyllites are indicated by grain size variations and/or change in mineral composition (Table 1). Slates and phyllites are characterized by varying degrees of cleavage development (see Table 1). Some of the slates and phyllites are characterized by two cleavage generations.

An Early Permian shale (P_1a_4, location #2/95) that occurs in the Pre-Uralian foredeep is characterized by quartz, albite and calcite as the major and illite and chlorite as the minor mineral phases (Fig. 4, Table 2). Carbonaceous slates of Upper Devonian age (D_3fm_1; Fig. 5; locations #1621, #1622, #1623, #1625) with quartz and chlorite as the major and illite as the minor mineral phases were studied in the Zilair nappe west of the Kraka nappe, and in its northern extension, the Tirlyan syncli-

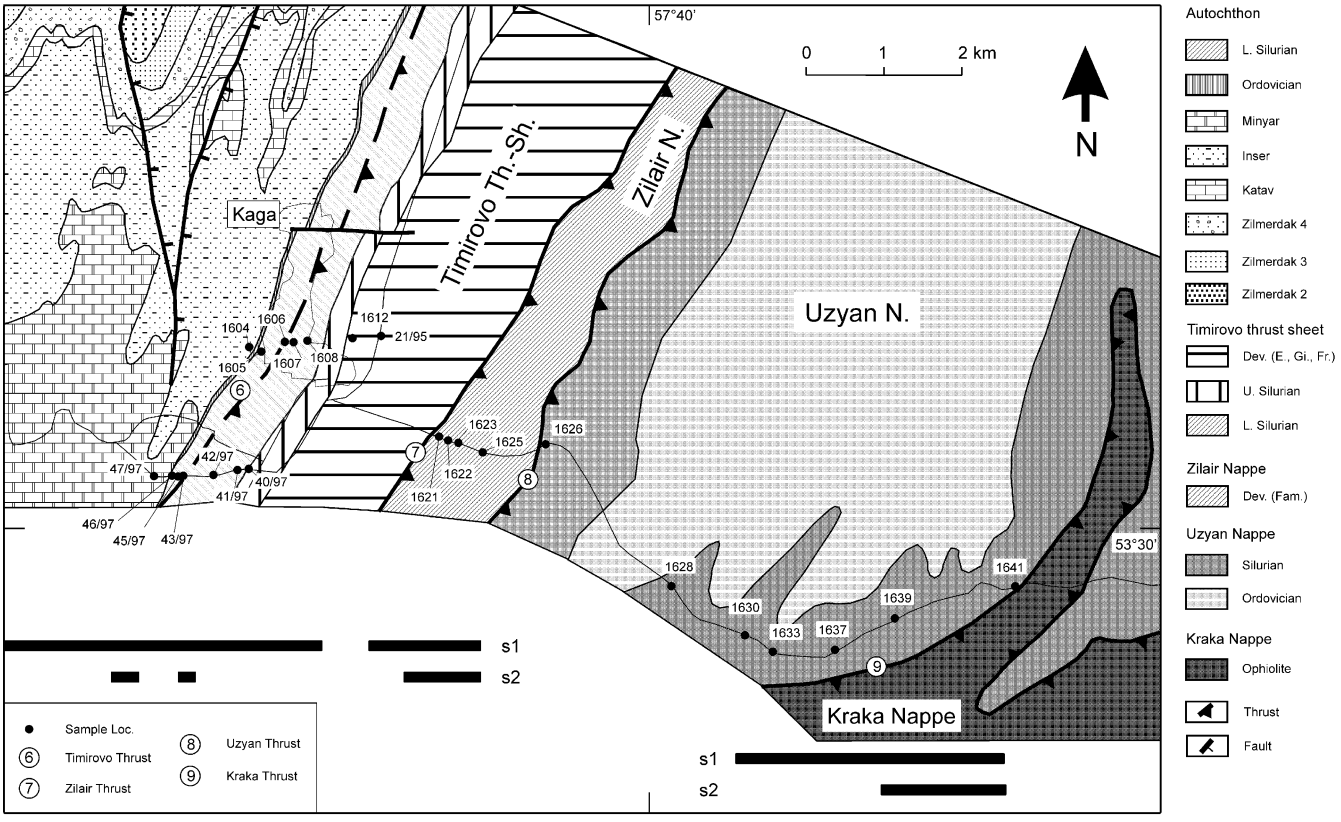

Fig. 5 Detailed geological map of the eastern stack of nappes in the footwall of the Main Uralian Fault (based on 1:50,000 scale maps). Shown are also the sample locations, sample location numbers and the cleavage. *s1* first cleavage; *s2* second cleavage

norium (locations #T2, #T3). Fine-grained muscovite is the main potassium bearing sheet silicate in a grey Upper Devonian slate of the Zilair nappe east of the Kraka nappe (location #90/97). Quartz is a major and illite and chlorite a minor component of the Lower Devonian shales (locations #1612, #21/95) of the Timirovo thrust sheet. Whereas albite was not detected in the Lower Devonian shales, albite occurs as an accessory to minor component in the Upper Devonian slates of the Zilair nappe. Shales and slates of Silurian age are only known from the Palaeozoic autochthon (locations #46/95, #45/95, #1605, #43/97), the Timirovo thrust sheet (locations #1606, #1607, #42/97, #1608, #41/97, #40/97) and the Uzyan nappe (locations #1626, #1628, #1630, #1633, #1637, #1639, #1641) east of the BMA. Quartz and illite are major and chlorite is a minor to accessory mineral component in the samples. Some of the samples are characterized by the occurrence of albite, anorthite and calcite in minor to accessory quantities.

The mineral composition of Vendian (locations #1502, #1509, #1538, #1515, #1518, #1523, #1525, #1529) and Upper Riphean (R_3, locations #1530, #1533, #1568, #1577, #25/97, #29/97, #47/97, #1604, DHK-1) shales, slates and phyllite is dominated by quartz, illite and partly chlorite. Feldspar (albite and/or potassium feldspar) and chlorite are minor components in shales and slates of both stratigraphic horizons. With increasing stratigraphic age (Middle and Lower Riphean, R_2 and R_1) illite is the major mineral phase in combination with quartz, chlorite. Fine-grained muscovite only occurs in Middle Riphean slates of the Yamantau anticlinorium.

Cleavage fabrics overprint the fine-grained sedimentary texture of the slates and phyllites (Table 1, Figs. 4 and 7). The intensity of the macroscopic cleavage increases from West to East. Only one black slate of the Ala-Tau anticlinorium (location #25/97) shows cleavage developed. The outcrop is located in the Zilmerdak thrust system and is characterized by steep isoclinal folds. The cleavage and the isoclinal folds are related to the thrust movement along the Zilmerdak thrust. In the western part of the Inzer synclinorium, no cleavage is developed. First cleavage planes occur within the Middle Riphean sedimentary units. The cleavage can be followed up to the Lower Devonian shale–limestone intercalation of the Timirovo Nappe. A second cleavage is developed in two locations (locations #1589, #1591) of the Inzer Synclinorium and one location (location #1583) in the Yamantau anticlinorium (Fig. 7). At location #1583, a black slate is crossed by a Precambrian magmatic dike (Alekseyev 1984). The sample was taken close to the dike. A less well-defined cleavage is developed in an outcrop (location #1585) about 1 km to the west. Black slates of the next outcrop to the east (location #1580, 4 km apart), which is located in the hanging wall of the main Avzyan thrust, shows a well-defined penetrative cleavage. Lower Silurian black slates of the Palaeozoic autochthon dis-

Table 1 Sample description. *L.-No.* location number; *S.-No.* sample number; *Stratigr.* stratigraphic position; *P* Permian; *PC* Precambrian; *S* Silurian; *LD* Lower Devonian; *UD* Upper Devonian; R_1js_2 Lower Riphean Jusha 2; R_1sr_2 Lower Riphean Suranjak 2; R_1sr_3 Lower Riphean Suranjak 3; R_1sr_4 Lower Riphean Suranjak 4; R_1sr_5 Lower Riphean Suranjak 5; R_2mh Middle Riphean Mashak; R_2av_1 Middle Riphean Lower Avzyan; R_2av_2 Middle Riphean Lower Avzyan; R_2av_4 Middle Riphean Upper Avzyan; R_3in Upper Riphean Inser; S_1w Silurian Wenlock; *ss* bedding; *s1* first cleavage; *s2* second cleavage; *g* grey; *d.g.* dark grey; *gr.* green; *b* black; *r.* red; *sh* shale; *sl* slate; *phy* phyllite; *n.a.* not analyzed

L.-No	S.-No.	Long.	Lat.	Stratigraphy		Lithology	ss	s1	s2
		(east)	(north)				(°)	(°)	(°)
Pre-Uralian foredeep									
2/95	2001	53°38.1′N	56°31.8′E	P	P_1a_4	d.g. sh.	240/36	no	No
Ala-Tau anticlinorium									
1502	2305	53°36.7′N	56°39.8′E	PC	Vzn	g. sh.	278/21	no	No
1509	2306	53°35.9′N	56°41.7′E	PC	Vbs	b. sh.	274/16	no	No
1538	2307	53°36.1′N	56°42.2′E	PC	Vbs	b. sh.	275/15	no	No
1515	2308	53°35.8′N	56°43.2′E	PC	Vbs	b. sh.	232/01	no	No
1518	2309	53°35.5′N	56°44.3′E	PC	Vbs	gr. sh.	146/07	no	No
1523	2310	53°35.8′N	56°46.5′E	PC	Vbs	g. sh.	318/06	no	No
1525	2311	53°35.6′N	56°47.5′E	PC	Vbs	g. sh.	312/11	no	No
1529	2312	53°35.5′N	56°48.6′E	PC	Vbs	g. sh.	097/22	no	No
1530	2313	53°35.4′N	56°48.8′E	PC	R_3zl_2	g. sh.	117/29	no	No
1533	2314	53°35.4′N	56°50.2′E	PC	R_3zl_2	g. sh.	094/28	no	No
1568	2315	53°33.8′N	57°03.8′E	PC	R_3in	g. sh.	078/25	no	No
1577	2316	53°33.6′N	57°08.3′E	PC	R_3in	g. sh.	110/37	no	No
25/97	2317	53°32.6′N	57°09.4′E	PC	R_3in	g. sl.	304/71	090/85	No
Inser synclinorium									
29/97	2318	53°32.1′N	57°10.3′E	PC	R_3zl_4	r. sh.	095/17	no	No
1589	2321	53°32.4′N	57°13.7′E	PC	R_2av_4	b. sl.	102/53	yes	yes
1591	2323	53°32.7′N	57°14.6′E	PC	R_2av_4	gr. sl.	334/36	099/44	yes
1595	2324	53°33.4′N	57°16.7′E	PC	R_2av_2	b. sl.	315/54	095/75	No
1587	2349	53°33.3′N	57°17.0′E	PC	R_2av_1	b. sl.	110/80	110/60	154/23
Yamantau anticlinorium									
1586	2348	53°33.3′N	57°17.5′E	PC	R_2av_1	b. sl.	285/65	yes	No
1585	2350	53°32.7′N	57°20.7′E	PC	R_1js_2	b. sl.	274/16	241/36	No
1584	2351	53°32.2′N	57°22.8′E	PC	R_1js_2	b. sl.	040/18	104/53	yes
1583	2352	53°32.1′N	57°23.0′E	PC	R_1js_2	b. sl.	047/45	076/66	yes
1580	2353	53°31.0′N	57°25.9′E	PC	R_2av_1	b. phy.	092/83	s1=ss	No
1579	2354	53°31.1′N	57°26.0′E	PC	R_2av_1	b. phy.	273/83	266/89	No
1598	2355	53°30.9′N	57°26.1′E	PC	R_2av_1	b. sl.	105/47	112/76	No
1599	2356	53°31.0′N	57°26.5′E	PC	R_2zk_3	b. sl.	105/35	S1=ss	No
1600	2357	53°31.0′N	57°27.3′E	PC	R_2zk_3	b. sl.	253/25	S1=ss	No
1601	2358	53°31.2′N	57°28.1′E	PC	R_2zk_3	b. sl.	128/44	yes	No
1602	2359	53°31.0′N	57°29.7′E	PC	R_2av_4	b. sl.	310/60	s1=ss	No
1603	2360	53°31.5′N	57°30.5′E	PC	R_2av_4	b. phy.	161/39	112/35	No
81/97	2339	53°32.7′N	57°31.6′E	PC	R_2av_1	b. phy.	188/34	90/75	No
79/97	2338	53°31.6′N	57°32.0′E	PC	R_2av_3	gr. phy.	138/55	114/80	No
75/97	2337	53°31.3′N	57°33.1′E	PC	R_2av_2	gr. phy.	266/63	105/70	No
47/97	2336	53°30.1′N	57°39.4′E	PC	R_3mn	gr. sl.	100/45	078/85	No
1604	2361	53°31.0′N	57°40.7′E	PC	R_3in	gr. sl.	228/22	287/85	242/34
Palaeozoic autochthon									
46/97	2335	53°30.0′N	57°39.4′E	S	S_1w	b. sl.	094/38	080/54	No
45/97	2334	53°30.2′N	57°39.8′E	S	S_1w	gr. sl.	102/37	092/63	No
1605	2362	53°31.1′N	57°40.6′E	S	S_1w	b. sl.	147/40	140/55	075/60
43/97	2332	53°30.2′N	57°40.0′E	S	S_1w	gr. sl.	085/58	088/71	No
Timirovo thrust sheet									
1606	2363	53°31.1′N	57°40.8′E	S	S_1w	b. sl.	108/59	100/78	107/67
1607	2364	53°31.2′N	57°41.1′E	S	S_1w	b. sl.	104/63	094/67	No
42/97	2331	53°30.3′N	57°40.1′E	S	S_1ld	gr. sl.	100/36	096/74	No
1608	2365	53°31.2′N	57°41.2′E	S	S_2ld	b. sl.	112/45	095/74	No
41/97	2330	53°30.3′N	57°44.2′E	S	S_1ld	gr. sl.	085/60	090/75	281/78
40/97	2329	53°30.3′N	57°40.3′E	S	S_2ld	dg. sl.	090/65	089/82	No
1612	2366	53°31.2′N	57°41.8′E	LD	D_2e_{vn}	g. sh.	108/72	no	No
21/95	2042	53°31.1′N	57°41.8′E	LD	D_2e_{vn}	g. sh.	119/40	no	No
Zilair nappe									
1621	2367	53°30.7′N	57°42.9′E	UD	D_3fm_1	b. sl.	272/43	102/28	No
1622	2368	53°30.6′N	57°42.9′E	UD	D_3fm_1	b. sl.	128/21	112/50	144/54
1623	2369	53°30.5′N	57°43.1′E	UD	D_3fm_1	b. sl.	100/20	105/40	Yes
1625	2370	53°30.5′N	57°43.4′E	UD	D_3fm_1	b. sl.	98/75	112/49	152/35

Table 1 (continued)

L.-No	S.-No.	Long. (east)	Lat. (north)	Stratigraphy		Lithology	ss (°)	s1 (°)	s2 (°)
Uzyan nappe									
1626	2046	53°30.6′N	57°43.5′E	S	S_1ln	b. sh.	128/40	no	No
1628	2372	53°29.5′N	57°45.4′E	S	S_1ln	b. sh.	141/66	no	No
1630	2373	53°29.2′N	57°56.0′E	S	S_1w	b. sl.	112/40	140/40	No
1633	2048	53°29.1′N	57°46.4′E	S	S_1w	b. sl.	118/31	252/28	No
1637	2374	53°29.1′N	57°46.8′E	S	?	b. sh.	116/75	yes	No
1639	2375	53°29.2′N	57°47.1′E	S	?	b. sl.	246/37	s1=ss	275/30
1641	2049	53°29.2′N	57°47.5′E	S	?	b. sh.	010/60	Thr: Serp. on Sil. cherts, Top to W, 094/29, shear fabric	
Zilair nappe (east of Kraka nappe)									
90/97	2340	53°29.3′N	58°01.3′E	UD	D_2fm_1	g. sl.	258/42	285/65	No
Zilair nappe (Tirlyan synclinorium)									
T2	2229	n.m.	n.m.	UD	D_2fm_1	b. sl.	yes	yes	n.m.
T3	2230	n.m.	n.m.	UD	D_2fm_1	b. sl.	yes	yes	n.m.
Drill hole Kulgunina 1 (second column is depth in m)									
DHK-1	1,122			PC	R_3Zl_1	r. sh.	n.a.	No	No
DHK-2	2,697			PC	R_2ZK	b. sh.	n.a.	No	No
DHK-3	3,534			PC	R_2js	b. sh.	n.a.	No	No
DHK-4	3,561			PC	R_{2j}s	b. sh.	n.a.	No	No
DHK-5	3,631			PC	R_{2j}s	b. sh.	n.a.	No	No
DHK-6	3,668			PC	R_{2j}s	b. sh.	n.a.	No	No
DHK-7	3,721			PC	R_{2j}s	b. sh.	n.a.	No	No
DHK-8	3,785			PC	R_{2j}s	b. sh.	n.a.	No	No
DHK-9	3,840			PC	R_{2j}s	b. sh.	n.a.	No	No
DHK-10	3,896			PC	R_{2j}s	b. sh.	n.a.	No	No
DHK-11	4,170			PC	R_{2j}s	b. sh.	n.a.	No	No

cordantly overly the Upper Riphean grey slates characterized by two distinct cleavages. Locally, a second cleavage is also developed in the Lower Silurian black slates. Two cleavage systems are developed in nearly all outcrops of the Upper Devonian black slates of the Zilair nappe. In addition, Silurian slates of the Uzyan nappe are cleaved. Parts of the samples show two cleavage planes.

Clay mineral composition and Kübler and Árkai indices

Illite and chlorite are the main mineral phases of the <2-μm-size fractions in all samples. Quartz only occurred as an accessory constituent. Feldspar was not detected by XRD analysis in any of the samples (detection limit 3%). Black to dark grey shales of the PUF (location #2/95), the Ala-Tau anticlinorium (locations #1568, #1577), the drill hole Kul 1 (DHK-2) and the Timirovo thrust sheet (locations #1612, # 21/95) bear various amounts of mixed layer minerals (I/S), indicating a lower degree of metamorphic overprint. The I/S also occurred in Silurian black slates of the easternmost location of the Uzyan nappe (location #1641). The latter slate is characterized by a homogeneous strong shear fabric (top to the west). Recrystallization of clay minerals during shear strain does not generate I/S. Therefore, we assume that the I/S might be of post-shear-deformation origin. Similarly, the I/S of a slate (locations #25/97) close to the Zilmerdak thrust, might also be of post-shear-deformation origin.

The Kübler indices along the URSEIS'95 transect and the KUL 1 drill hole range from lower late diagenesis [CIS-$FWHM_{ill001ad}$=0.792 (28) °Δ2ΘCuKα] in an Upper Riphean shale (#2316) of the Ala-Tau anticlinorium (ATA) to epizonal values [CIS-$FWHM_{ill001ad}$=0.210 (0) °Δ2ΘCuKα] in Middle Riphean slates (#2337) of the Yamantau anticlinorium (YA; Table 3). Further to the east, lower late diagenetic grade are only indicated by the Kübler index of a Lower Devonian shale (#2366) in the Timirovo thrust sheet. The Árkai indices could only be determined for 35 of the 71 samples and ranges from diagenesis [CIS-$FWHM_{chl002ad}$=0.400 (12) °Δ2ΘCuKα] in Vendian shales of the ATA to epizonal values [CIS-$FWHM_{chl002ad}$=0.253 (8) °Δ2ΘCuKα] in Precambrian slates of the YA. With the exception of samples that bear I/S, both parameters correlate well (Fig. 8a). Nearly all Precambrian shales of diagenetic grade as revealed by CIS-$FWHM_{ill001ad}$ are characterized by an Árkai index of anchizonal grade. This discrepancy might either indicate a detrital origin of chlorite or a strong influence of detrital chlorite grains.

Local misfits of both parameters can be seen in the absolute values, the CIS-$FWHM_{Chl002ad}$ values of slates and phyllites frequently indicating lower and higher metamorphic grades. As discussed by Merriman and Peacor (1999), chlorite crystals growing under high strain rates are commonly characterized by subgrain boundaries and dislocations and, consequently, by a reduced crystallite thickness. In comparison to white mica, significant dif-

Table 2 Mineral composition of <63 m-size fraction. *XX* major =>20%; *X* minor =<20%; *ac* accessory =<5%; - not detected; *An* anorthite; *w-M* white mica with the exception of illite

L.-No.	S.-No.	Strat.	Qtz	K-Fsp	Alb	An	w-M	Ill	Chl	Cal	Hem
Pre-Uralian foredeep											
2/95	2001	P_1a_1	xx	-	x	-	-	x	x	xx	-
Ala-Tau anticlinorium											
1502	2305	Vzn	xx	-	x	-	-	x	x	-	-
1509	2306	Vbs	xx	-	x	-	-	x	x	-	-
1538	2307	Vbs	xx	-	x	-	-	x	x	-	-
1515	2308	Vbs	xx	-	-	-	-	xx	xx	-	-
1518	2309	Vbs	xx	-	-	-	-	xx	x	-	-
1523	2310	Vbs	x	-	-	-	-	xx	xx	-	ac
1525	2311	Vbs	xx	-	-	-	-	xx	x	-	-
1529	2312	Vbs	xx	-	x	-	-	xx	x	-	ac
1530	2313	R_3zl_2	xx	-	x	-	-	x	x	-	ac
1533	2314	R_3zl_2	xx	x	x	-	-	x	ac	-	ac
1568	2315	R_3in	xx	-	x	-	-	x	x	-	-
1577	2316	R_3in	xx	-	-	-	-	xx	-	-	-
25/97	2317	R_3in	xx	-	x	-	-	x	ac	-	-
Inser synclinorium											
29/97	2318	R_3zl_4	xx	x	-	-	-	xx	ac	-	x
1589	2321	R_2av_4	xx	-	-	-	-	x	x	-	-
1591	2323	R_2av_4	xx	-	-	-	-	x	x	-	-
1595	2324	R_2av_2	xx	-	x	-	-	xx	x	-	-
1587	2349	R_2av_1	xx	ac	ac	-	-	xx	x	ac	-
Yamantau anticlinorium											
1586	2348	R_2av_1	xx	ac	-	-	-	xx	-	-	-
1585	2350	R_1js_2	xx	ac	x	-	-	xx	x	-	-
1584	2351	R_1js_2									
1583	2352	R_1js_2	xx	ac	x	-	-	xx	ac	-	-
1580	2353	R_2av_1	xx	ac	ac	-	xx	-	-	-	-
1579	2354	R_2av_1	xx	x	ac	-	xx	-	-	-	-
1598	2355	R_2av_1	xx	-	-	-	-	x	-	x	-
1599	2356	R_2zk_3	xx	x	ac	-	-	xx	-	-	-
1600	2357	R_2zk_3	xx	-	ac	-	-	x	x	-	-
1601	2358	R_2zk_3	xx	-	ac	-	-	xx	x	-	-
1602	2359	R_2av_4	xx	-	ac	-	x	x	-	-	-
1603	2360	R_2av_4	xx	-	ac	-	xx	-	ac	-	-
81/97	2339	R_2av_1	xx	ac	ac	-	x	-	x	ac	-
79/97	2338	R_2av_3	xx	-	x	-	xx	-	ac	ac	-
75/97	2337	R_2av_2	xx	-	x	-	xx	-	x	-	-
47/97	2336	R_3mn	xx	-	-	-	-	x	x	-	-
1604	2361	R_3in	xx	-	-	-	-	x	x	-	-
Palaeozoic autochthon											
46/97	2335	S_1w	xx	-	ac	-	-	xx	x	x	-
45/97	2334	S_1w	xx	-	-	-	-	xx	x	-	-
1605	2362	S_1w									
43/97	2332	S_1w	xx	-	-	ac	-	xx	x	-	-
Timirovo thrust sheet											
1606	2363	S_1w									
1607	2364	S_1w									
42/97	2331	S_2ld	xx	-	-	ac	-	xx	x	-	-
1608	2365	S_2ld	xx	-	ac	-	-	xx	x	-	-
41/97	2330	S_2ld	xx	-	-	-	-	xx	x	-	-
40/97	2329	S_2ld	xx	-	-	-	-	xx	x	-	-
1612	2366	D_2e_{vn}									
21/95	2042	D_2e_{vn}	xx	-	-	-	-	x	x	-	-
Zilair nappe (west of Kraka nappe)											
1621	2367	D_3fm_1	xx	-	ac	-	-	x	xx	-	-
1622	2368	D_3fm_1	xx	-	ac	-	-	x	xx	-	-
1623	2369	D_3fm_1	xx	-	ac	-	-	x	xx	-	-
1625	2370	D_3fm_1	xx	-	ac	-	-	x	xx	-	-
Uzyan nappe											
1626	2046	S_1ln	xx	-	-	x	-	xx	-	-	-
1628	2372	S_1ln									
1630	2373	S_1w	xx	-	-	-	-	xx	ac	-	-
1633	2048	S_1w	xx	-	-	x	-	xx	-	-	-
1637	2374	S.									
1639	2375	S.	xx	-	-	-	-	xx	x	-	-
1641	2049	S.									

Table 2 (continued)

L.-No.	S.-No.	Strat.	Qtz	K-Fsp	Alb	An	w-M	Ill	Chl	Cal	Hem
Zilair nappe (east of Kraka nappe)											
90/97	2340	D_2fm	xx	-	x	-	x	-	xx	-	-
Zilair nappe (Tirlyan synclinorium)											
T2	2229	D_2fm_1	xx	-	x	-	-	x	xx	-	-
T3	2230	D_2fm_1	xx	-	x	-	-	x	xx	-	-
Drill hole Kulgunina 1 (second column is depth in m)											
DHK-1	1,122	R_3Zl_1	xx	x	x	-	-	x	-	-	x
DHK-2	2,697	R_2ZK	xx	x	-	-	-	x	-	-	-
DHK-3	3,534	R_2js	xx	-	ac	-	-	x	x	-	-
DHK-4	3,561	$R_{2j}s$	xx	-	ac	-	-	x	x	-	-
DHK-5	3,631	$R_{2j}s$	xx	-	ac	-	-	x	x	-	-
DHK-6	3,668	$R_{2j}s$	xx	-	ac	-	-	x	xx	-	-
DHK-7	3,721	$R_{2j}s$	x	-	-	-	-	x	xx	-	-
DHK-8	3,785	$R_{2j}s$	xx	-	ac	-	-	x	xx	-	-
DHK-9	3,840	$R_{2j}s$	xx	-	-	-	-	x	xx	-	-
DHK-10	3,896	$R_{2j}s$	xx	-	-	-	-	x	xx	-	-
DHK-11	4,170	$R_{2j}s$	xx	-	ac	-	-	x	xx	-	-

ferences in index values result in better Kübler than Árkai indices where low-grade metamorphism is associated with the development of tectonic fabrics. However, Wang et al. (1996) described enhanced Árkai indices relative to the Kübler indices in deformed pelitic rocks. Nearly all slates and phyllites of the URSEIS'95 and KUL 1 drill hole are characterized by enhanced Kübler indices. The internal deformation indicated by the presence of a cleavage does lead to decrease in Árkai indices.

In order to qualitatively describe the I/S, air-dried samples were glycolated and the Kübler and Árkai indices determined again (Figs. 8b, c). Lower late diagenetic shales are characterized by a noticeable content of expandable mineral phases. Towards the diagenesis–anchizone boundary, the amount of I/S decreases (Fig. 8b, c). Samples with CIS-$FWHM_{Ill001ad}$ values lower than 0.42 [°$\Delta 2\Theta$CuKα] and CIS-$FWHM_{Ch002ad}$ values lower than 0.33 [°$\Delta 2\Theta$CuKα] show negligible variations after glycolation.

Diagenetic grades are typical for the Early Permian shales of the Pre-Uralian Foredeep (Fig. 9). East of the Tashli thrust, which separates the Pre-Uralian Foredeep from the Ala-Tau anticlinorium, the Kübler indices indicates middle anchizonal grades [CIS-$FWHM_{ill001ad}$ 0.347 (41) °$\Delta 2\Theta$CuKα]. With increasing distance, the Kübler indices of the Vendian shales decrease to the anchizonal/diagenesis boundary. The Kübler indices do not show variation with stratigraphic age of the Vendian shales. The Árkai indices indicate, for nearly all samples between Tashli thrust and Alatau thrust, a finite metamorphic grade at the anchizone/diagenesis boundary. East of the Alatau thrust, the Kübler indices of Upper Riphean shales (Zilmerdak unit: 950 Ma; Semikhatov et al. 1991) decrease to late diagenetic grades. Furthermore, Upper Riphean shales (Inzer unit: 850 Ma; Semikhatov et al. 1991) in the eastern part of the Ala-Tau anticlinorium, close to the Zilmerdak thrust, are characterized by lower late diagenetic grades. In the central part of the Ala-Tau anticlinorium, the 5,142-m-deep drill hole Kul 1 penetrated Upper and Middle Riphean sedimentary units (Fig. 6). Because numerous diabase and syenite dikes occur in the middle part of the drill hole, samples were taken mostly in the lower part of the drill core (3,140–4,696 m). The Kübler index values vary strongly in the diagenetic field, but a general tendency of decreasing values occurred from about 3,000 to 4,500 m. Only two samples reached anchizonal/diagenesis boundary grades. The Árkai indices indicates anchizonal grades. The minor variability of the Árkai indices in relation to the Kübler indices might be indicative for a partly or complete detrital origin of the chlorite grains.

In the Inzer synclinorium, east of the east dipping Zilmerdak thrust and west of the westernmost thrust of the east dipping Avzyan thrust zone, the Kübler indices increase from late diagenetic grades to middle anchizonal values (Fig. 10). The increase in finite metamorphic grade is accompanied by the occurrence of the first cleavage (s1). Upper Riphean slates of the Inzer synclinorium show consistently increasing Kübler indices into stratigraphical older rocks (Table 3, Fig. 10).

In the western part of the Yamantau anticlinorium, the Kübler index values keep nearly constant at the anchizone/diagenesis boundary in Lower Riphean sedimentary rocks (Fig. 10). One exceptional value at the anchizone/epizone boundary was revealed from a black slate in the wall rock of a thick Precambrian diabase dike (Alekseyev 1984) and might, therefore, be of Precambrian age. Entering the Middle to Lower Riphean strata of the Yamantau anticline by passing the main Avzyan thrust (Figs. 10 and 11), the value of CIS-$FWHM_{ill001ad}$ diminishes from 0.450 (53) °$\Delta 2\Theta$CuKα (upper diagenesis) to 0.244 (0) °$\Delta 2\Theta$CuKα (epizone). A slight increase in the Kübler index value occurs in the hanging wall of the easternmost thrust of the Avzyan thrust system. Árkai et al. (1997) describe, in the hanging wall of the Glarus thrust plane in the Swiss Helvetic Alps, a decrease in illite crystallite size. They suggest that strain-induced reduction in illite crystallite size resulted from intracrystal slip and

Table 3 Kübler and Árkai indices of the <2-m-size fraction. *ICad* CIS-FWHM$_{Ill001ad}$= Kübler index air dried; *ICgly* CIS-FWHM$_{Ill001gly}$=Kübler index glycolated; *ChCad* CIS-FWHM$_{Chl002ad}$=Árkai index air dried; *ChCgly* CIS-FWHM$_{Chl002gly}$=Árkai index glycolated; *std*. standard deviation is related to repeated measurement of the same sample

Location	Sa.	Strat.	ICad (1std)	ICgly (1std)	ChCad (1std)	ChCgly (1std)
No.	No.	Pos.	[°Δ2ΘCuKα]	[°Δ2ΘCuKα]	[°Δ2ΘCuKα]	[°Δ2ΘCuKα]
Pre-Uralian Foredeep						
2/95	2001	P_1a_1	0.753 (71)	0.627 (83)	-	-
Ala-Tau Anticlinorium						
1502	2305	Vzn	0.347 (41)	0.347 (16)	0.400 (12)	0.389 (14)
1509	2306	Vbs	0.347 (27)	0.381 (16)	0.336 (13)	0.349 (15)
1538	2307	Vbs	0.416 (17)	0.381 (31)	0.325 (22)	0.317 (13)
1515	2308	Vbs	0.381 (31)	0.381 (16)	0.325 (0)	0.309 (7)
1518	2309	Vbs	0.416 (34)	0.347 (16)	0.333 (19)	0.325 (11)
1523	2310	Vbs	0.381 (16)	n.a.	0.333 (13)	n.a.
1525	2311	Vbs	0.416 (28)	0.416 (16)	0.357 (24)	0.341 (17)
1529	2312	Vbs	0.416 (35)	0.450 (31)	0.301 (23)	0.325 (40)
1530	2313	R_3zl_2	0.484 (25)	0.450 (41)	0.317 (16)	0.309 (14)
1533	2314	R_3zl_2	0.484 (95)	0.484 (30)	-	-
1568	2315	R_3in	0.621 (21)	0.484 (17)	0.373 (18)	0.325 (15)
1577	2316	R_3in	0.792 (28)	0.724 (40)	-	-
25/97	2317	R_3in	0.621 (61)	0.553 (37)	-	-
Inser synclinorium						
29/97	2318	R_3zl_4	0.473 (21)	0.484 (31)	-	-
1589	2321	R_2av_4	0.450 (17)	0.416 (23)	-	-
1591	2323	R_2av_4	0.416 (27)	0.347 (0)	0.277 (18)	0.285 (9)
1595	2324	R_2av_2	0.381 (27)	0.381 (16)	0.330 (36)	0.290 (24)
1587	2349	R_2av_1	0.347 (27)	0.347 (16)	0.317 (20)	0.317 (13)
Yamantau anticlinorium						
1586	2348	R_2av_1	0.416 (26)	0.416 (27)	-	-
1585	2350	R_1js_2	0.450 (16)	0.450 (16)	-	-
1584	2351	R_1js_2	0.450 (53)	0.416 (28)	-	-
1583	2352	R_1js_2	0.279 (0)	0.279 (0)	-	-
1580	2353	R_2av_1	0.244 (0)	0.244 (0)	-	-
1579	2354	R_2av_1	0.244 (0)	0.244 (0)	-	-
1598	2355	R_2av_1	0.261 (16)	0.279 (0)	-	-
1599	2356	R_2zk_3	0.279 (16)	0.279 (0)	-	-
1600	2357	R_2zk_3	0.279 (31)	0.279 (0)	-	-
1601	2358	R_2zk_3	0.279 (10)	0.279 (0)	-	-
1602	2359	R_2av_4	0.278 (16)	0.244 (0)	-	-
1603	2360	R_2av_4	0.244 (0)	0.244 (0)	-	-
81/97	2339	R_2av_1	0.244 (0)	0.244 (0)	0.267 (7)	0.261 (7)
79/97	2338	R_2av_3	0.244 (0)	0.244 (0)	-	-
75/97	2337	R_2av_2	0.210 (0)	n.a.	0.253 (8)	n.a.
47/97	2336	R_3mn	0.279 (16)	0.279 (16)	0.357 (15)	0.325 (25)
1604	2361	R_3in	0.279 (0)	0.279 (0)	0.277 (11)	0.285 (8)
Palaeozoic autochthons						
46/97	2335	S_1w	0.518 (24)	0.553 (31)	-	-
45/97	2334	S_1w	0.518 (16)	0.484 (39)	-	-
1605	2362	S_1w	0.484 (16)	0.450 (16)	0.373 (8)	0.355 (27)
43/97	2332	S_1w	0.450 (16)	0.416 (39)	-	-
Timirovo thrust sheet						
1606	2363	S_1w	0.381 (16)	0.381 (14)	0.341 (12)	0.355 (14)
1607	2364	S_1w	0.381 (16)	0.347 (0)	0.357 (20)	0.341 (22)
42/97	2331	S_2ld	0.381 (28)	0.381 (16)	-	-
1608	2365	S_2ld	0.381 (14)	0.381 (0)	-	-
41/97	2330	S_2ld	0.450 (31)	0.416 (31)	-	-
40/97	2329	S_2ld	0.450 (16)	0.450 (16)	-	-
1612	2366	D_2e_{vn}	0.724 (29)	0.598 (58)	-	-
21/95	2042	D_2e_{vn}	0.556 (30)	0.386 (110)	-	-
Zilair nappe (west of Kraka nappe)						
1621	2367	D_3fm_1	0.416 (0)	0.381 (16)	-	-
1622	2368	D_3fm_1	0.279 (16)	0.313 (16)	0.277 (7)	0.277 (7)
1623	2369	D_3fm_1	0.313 (16)	0.347 (16)	0.285 (15)	0.285 (8)
1625	2370	D_3fm_1	0.313 (17)	0.347 (16)	0.293 (0)	0.293 (0)
Uzyan nappe						
1626	2046	S_1ln	0.391 (14)	0.360 (15)	-	-
1628	2372	S_1ln	0.450 (21)	0.450 (41)	-	-
1630	2373	S_1w	0.416 (17)	0.416 (16)	-	-
1633	2048	S_1w	0.548 (52)	0.579 (52)	-	-
1637	2374	S.	0.244 (0)	0.244 (0)	-	-
1639	2375	S.	0.450 (27)	0.450 (12)	-	-
1641	2049	S.	0.642 (55)	0.548 (34)	-	-

Table 3 (continued)

Location No.	Sa. No.	Strat. Pos.	ICad (1std) [°Δ2ΘCuKα]	ICgly (1std) [°Δ2ΘCuKα]	ChCad (1std) [°Δ2ΘCuKα]	ChCgly (1std) [°Δ2ΘCuKα]
Zilair nappe (east of Kraka nappe)						
90/97	2340	D_3fm_1	0.244 (0)	0.244 (0)	0.261 (7)	0.261 (0)
Zilair nappe (east of Kraka nappe)						
T2	2229	D_3fm_1	0.278 (16)	0.243 (0)	0.244 (0)	0.260 (0)
T3	2230	D_3fm_1	0.278 (0)	0.278 (16)	0.260 (0)	0.260 (7)
Drill hole Kulgunina 1 (second column is depth in m)						
DHK-1	1,122	R_3Zl_1	0.621 (20)	0.636 (45)	-	-
DHK-2	2,697	R_2ZK	0.747 (34)	0.668 (33)	-	-
DHK-3	3,534	R_2js	0.563 (21)	0.542 (33)	0.340 (11)	0.340 (11)
DHK-4	3,561	$R_{2j}s$	0.518 (14)	0.553 (37)	0.340 (11)	0.340 (11)
DHK-5	3,631	$R_{2j}s$	0.690 (20)	0.690 (27)	0.308 (22)	0.324 (17)
DHK-6	3,668	$R_{2j}s$	0.518 (28)	0.484 (48)	0.308 (6)	0.292 (0)
DHK-7	3,721	$R_{2j}s$	0.450 (24)	0.381 (47)	0.308 (7)	0.308 (0)
DHK-8	3,785	$R_{2j}s$	0.450 (49)	0.398 (16)	0.292 (13)	0.300 (8)
DHK-9	3,840	$R_{2j}s$	0.551 (15)	0.508 (25)	0.308 (8)	0.284 (13)
DHK-10	3,896	$R_{2j}s$	0.416 (34)	0.381 (44)	0.300 (8)	0.308 (7)
DHK-11	4,170	$R_{2j}s$	0.518 (27)	0.450 (35)	0.292 (0)	0.300 (8)

subgrain formation. Therefore, the value in the hanging wall of the eastern most Avzyan thrust of the Avzyan thrust system is unlikely to represent a metamorphic grade. Close to the discordance of the Palaeozoic autochthonous sedimentary units the Kübler indices decrease to upper anchizonal values [CIS-$FWHM_{ill001ad}$ 0.279 (16) °Δ2ΘCuKα] in Upper Riphean slates. These slates are characterized by two generations of cleavage fabric.

The western limb of the Zilair synclinorium consists of Lower Palaeozoic siliciclastic and carbonate rocks that unconformably overlap the Precambrian basement of the Bashkirian Mega-anticlinorium. The autochthonous Palaeo-zoic units are overlain by a stack of thrust sheet and nappes (Fig. 10). The Kübler indices drastically decrease from upper anchizonal values of the Upper Riphean slates to middle diagenetic values of the autochthonous Silurian slates. Within the autochthonous Palaeozoic cover, the Kübler indices increase from upper diagenesis [CIS-$FWHM_{ill001ad}$ 0.518 (24) °Δ2ΘCuKα] to the anchizone/diagenesis boundary in the vicinity of the Timirovo thrust.

The Timirovo thrust separates the Palaeozoic autochthonous cover and the Silurian to Lower Devonian sediments of the Timirovo thrust sheet. The Kübler indices consistently decrease from lower anchizonal [CIS-$FWHM_{ill001ad}$ 0.381 (16) °Δ2ΘCuKα] to lower late diagenetic [CIS-$FWHM_{ill001ad}$ 0.724 (29) °Δ2ΘCuKα] values into stratigraphical younger rocks (Fig. 10).

An increase of the Kübler indices towards anchizonal values occurred in the Zilair nappe, the next nappe to the east. The Upper Devonian black slates of the Zilair nappe are dominated by CIS-$FWHM_{ill001ad}$ values of the upper anchizone [0.313 (16) °Δ2ΘCuKα]. Only one slate revealed a Kübler index value close to the anchizone/diagenesis boundary. This sample is the black slate with only one cleavage.

At the Uzyan thrust that separates the Upper Devonian siliciclastic units of the Zilair nappe from the Silurian units of the Uzyan nappe, the Kübler indices change from upper anchizonal values of the Upper Devonian slates to values at the anchizone/diagenesis boundary of the Silurian shales. Within the Uzyan nappe the Kübler index, values vary between lower anchizone and lower late diagenesis. East of the Kraka nappe, the Kübler indices of black slates indicate epizonal grades.

The Árkai indices show general congruence with CIS-$FWHM_{ill001ad}$ measurements for the high- and low-grade regions of the URSEIS'95 transect. In areas of higher metamorphic grade like the Yamantau anticline and Zilair nappe, the Árkai indices yield results similar to the Kübler indices reflecting upper anchi- to epizonal grades. As described by Árkai et al. (1995) "the ChC method is less sensitive for identifying differences in metamorphic grade than the IC method" for regions of very low metamorphic grade. Our experiences in the ATA, the Kul 1 drill hole and the Inzer synclinorium clearly confirm this statement.

Discussion

Discussion and interpretation of the Kübler and Árkai indices have to consider their spatial distribution and the textural evolution of the samples. Including the diagenetic to incipient metamorphic data of the AC-TS'96 transect (Matenaar et al. 1999), the study of the western fold-and-thrust belt of the southern Urals outlines a general increase of metamorphic grade and intensity of cleavage from west to east (Fig. 11).

Pre-Uralian Foredeep

In the Pre-Uralian foredeep, the Kübler and Árkai indices and vitrinite reflectance values (AC-TS'96, Matenaar et al. 1999) indicate a lower late diagenetic stage. According to Merriman and Frey (1999) such a diagenetic stage would account for more than 100 °C temperature. Apatite fission-track data of Early Permian sandstones and con-

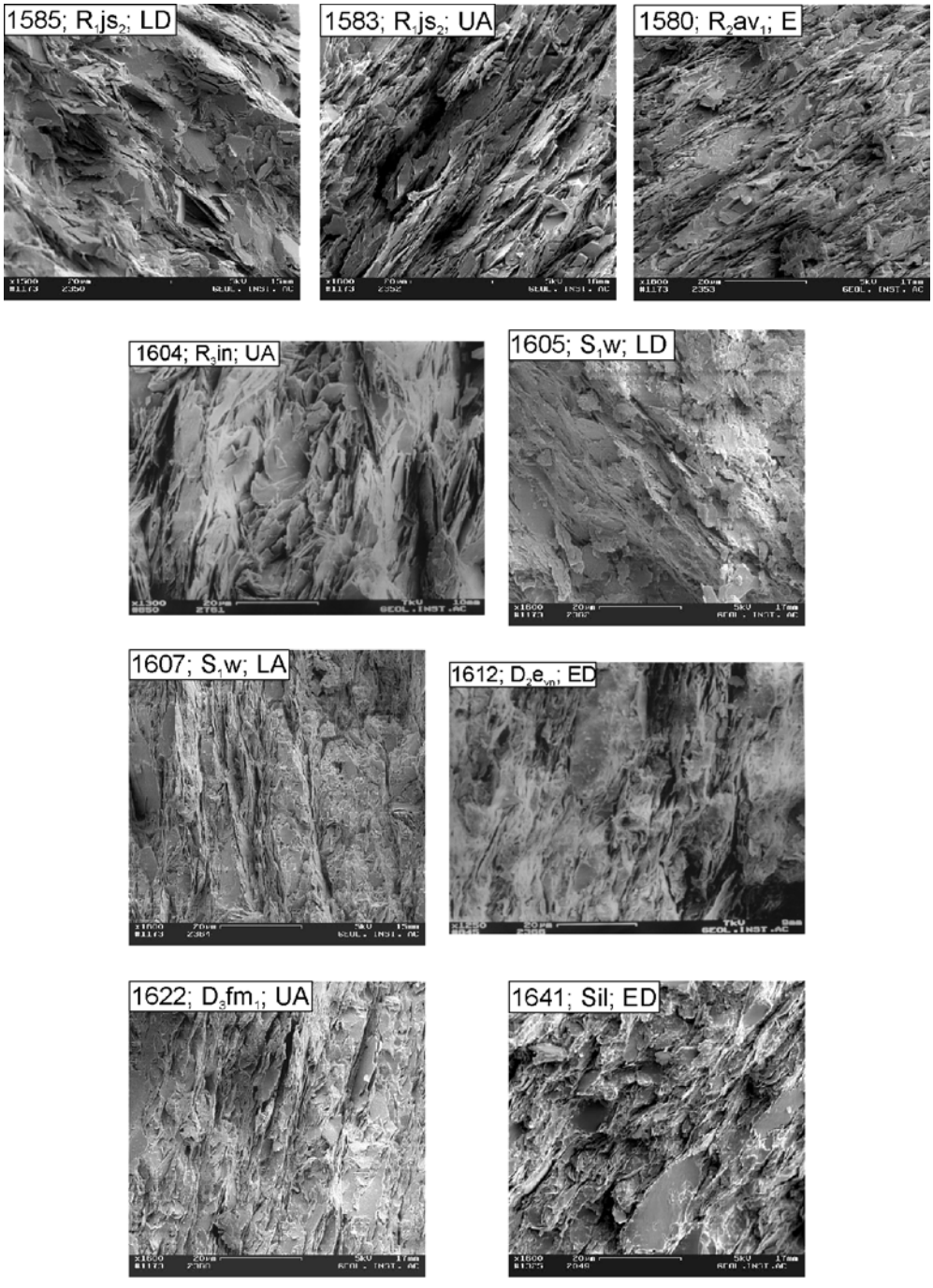

Fig. 6 SEM images of selected slates and phyllites from various locations along the URSEIS'95 transect. The images display various degrees of cleavage development. All images are taken with the same magnification. See text for further explanation. *1585* Sample number; *R1js2* stratigraphic position; *ED* early diagenesis; *LD* late diagenesis; *LA* lower anchizone; *UA* upper anchizone; *E* epizone

glomerates, presented by Glasmacher et al. (2002), indicate that detrital fission-track ages were only partly reset. Partial resetting of fission-track ages occur at temperatures below about 110 °C. These contradicting results indicate that the Kübler and Árkai indices and the vitrinite reflectance values reflect a mixture of grains and particles evolved during diagenesis and of detrital origin.

Ala-Tau Anticlinorium

At the Tashli thrust, the metamorphic grade increase to the middle anchizone. This increase could be attributed to the significant change of stratigraphic age (Upper Vendian) and would, therefore, indicate a pre-deformational origin. Further to the east, between Tashli and Alatau thrust, the metamorphic grade decreases continuously with final values reaching the diagenesis/anchizone boundary. The stronger increase in temperature close to the Tashli fault might be related to a thick Palaeozoic cover. Puchkov (2000) discussed the possibility of Early

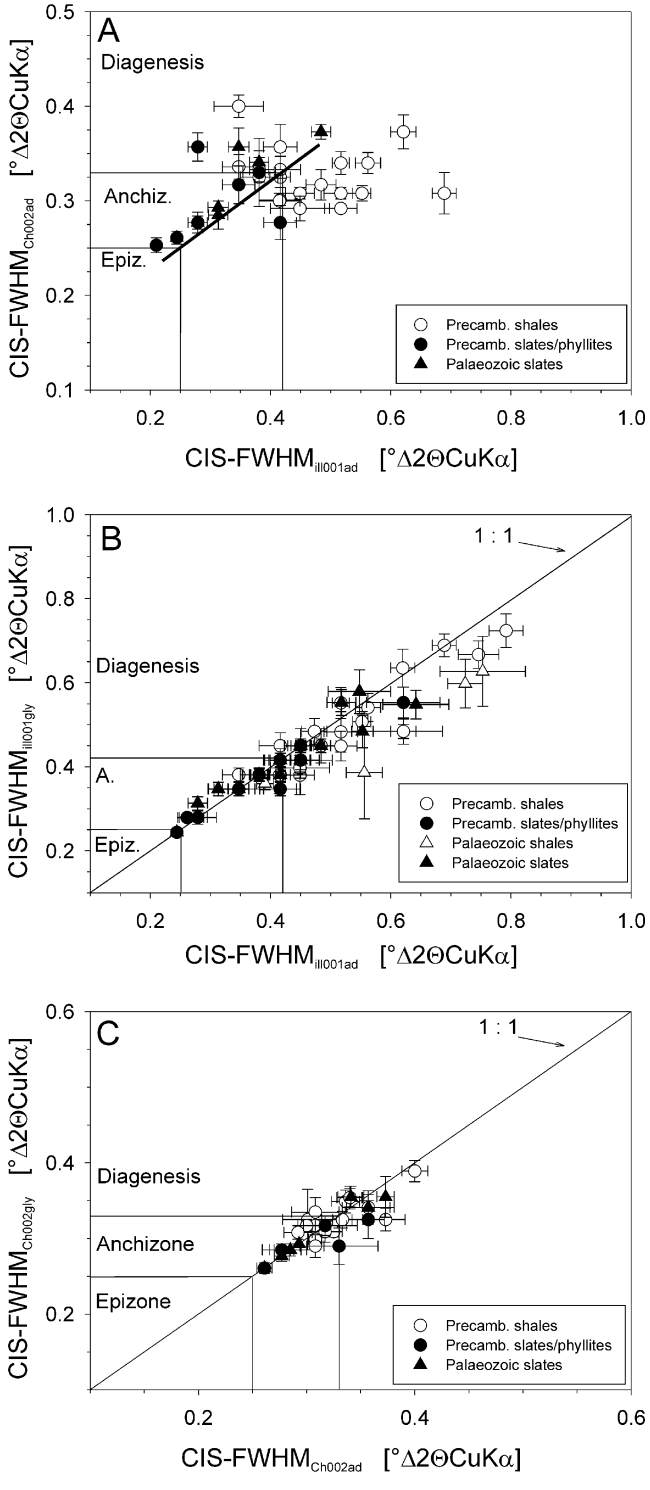

Fig. 7 Comparison between Kübler indices (CIS-FWHM$_{Ill001ad}$± std. dev.) and Árkai indices (CIS-FWHM$_{Chl002ad}$±std. dev.). **B** Comparison of Kübler indices before (CIS-FWHM$_{Ill001ad}$±std. dev.) and after (CIS-FWHM$_{Ill001gly}$±std. dev.) glycolation. **C** Comparison of Árkai indices before (CIS-FWHM$_{Chl002ad}$±std. dev.) and after (CIS-FWHM$_{Chl002gly}$±std. dev.) glycolation

Permian siliciclastic sedimentary rocks overlying the Devonian to Carboniferous carbonate sequence in the western part of the Ala-Tau anticlinorium. This sedimentary sequence reaches a total thickness of about 4,000 m. Based on apatite fission-track data along the AC-TS'96 transect, Glasmacher et al. (2002) assumed a palaeo-temperature gradient of about 27 °C/km in Permian time around the Tashli fault. It cannot be excluded that the heat flow might be local, has a hydrothermal component and is related to the Tashli fault. In addition, the $^{40}Ar/^{39}Ar$ spectra of microcline from an Upper Vendian conglomerate close to the Tashli fault at the AC-TS'96 indicates that the Vendian conglomerate was heated sufficiently (>140 °C) to partly reset the $^{40}Ar/^{39}Ar$-system of microcline in Palaeozoic time (Glasmacher et al. 2001).

Along the URSEIS'95 transect, the apatite fission-track data of Lower Devonian and Vendian sandstones are completely reset east of the Tashli fault (Fig. 3; Seward et al. 1997). To completely reset the detrital fission-track signature of apatite grains, a temperature of more than 110 °C at the geological time scale is needed. The middle anchizonal grades of the Upper Vendian shales in the western part of the Ala-Tau anticlinorium indicate a temperature of more than 200 °C. The fission-track age [401(71)] of zircon from an Upper Vendian sandstone (~600 Ma) suggests a partial annealing of the fission-tracks (Seward et al. 1997). As shown by Kasuya and Naeser (1988), annealing of fission-tracks in zircon is a function of temperature, time and α-radiation damage. The amount of α-radiation damage increases with time and with uranium and thorium concentration in zircon. Tagami and Shimada (1996), from studying a zircon fission-track system around a granitic pluton, envisaged a zircon partial annealing zone (ZPAZ) of between ~230 and 320 °C for a heating duration of about 10^6 years. Fission-tracks in zircon grains from Miocene to Pleistocene sandstones and Miocene to Pliocene rhyolites of two drill holes in a sedimentary basin in Japan give indications for a temperature above 200 °C as the lower limit of the ZPAZ for temperature stability of about 1 Ma (Hasebe et al. 2003). Furthermore, results of laboratory annealing experiments point towards a similar temperature range of the ZPAZ (Yamada et al. 1995; Tagami et al. 1998). Fission-tracks in zircon grains with high α-radiation damage start to anneal at temperatures of between 150 and 200 °C (Graver 2001; Riley 2002). The temperature range of the ZPAZ adequately covers the anchi- to epizone. Based on the above described temperature range for the ZPAZ, the partially reset fission-track age of zircon [401(71)] from an Upper Vendian sandstone further supports a middle anchizonal incipient metamorphic grade for the western Ala-Tau anticlinorium. Applying a palaeo-temperature gradient of about 27 °C/km as assumed for the northern transect by Glasmacher et al. (2002), a thickness of more than 7,000 m would be necessary to account for the anchizonal grade. The Devonian, Carboniferous and lowermost part of the Early Permian sedimentary sequence along the UR-

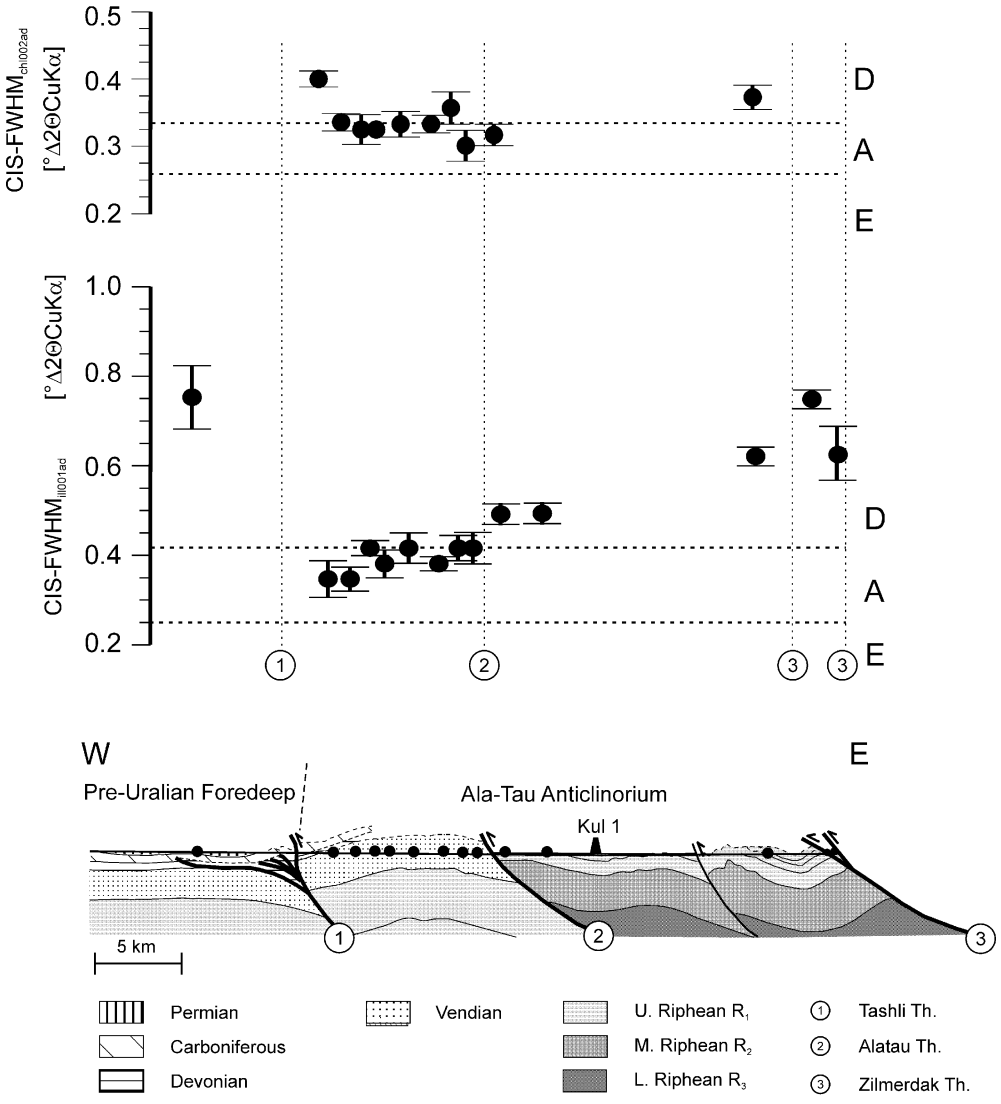

Fig. 8 Comparison of Kübler and Árkai indices from the Pre-Uralian foredeep and the Ala-Tau anticlinorium. *D* diagenesis; *A* anchizone; *E* epizone

SEIS'95 transect reaches an overall thickness of about 5,000 m. Therefore, it has to be considered that either a significant amount of Upper Vendian strata is needed to account for the missing thickness, or the palaeo-temperature gradient was more than 30 °C/km.

Along the URSEIS'95 transects the eastern part of the Ala-Tau anticlinorium that consists mainly of Upper Riphean sediments is characterized by a lower late to upper late diagenetic grade. Such a low grade does not allow a thick sedimentary cover of Vendian and Palaeozoic age. According to Puchkov (2000) and Kozlov et al (1995), the Devonian to Carboniferous sequence reached a thickness of about 2,500 m. The increase of metamorphic grade with depth in the Kul 1 drill hole close to the URSEIS'95 transect reached grades at the diagenesis/anchizonal boundary (about 200 °C, Merriman and Frey 1999) at a depth of about 3,900 m (Lower Riphean Yusha formation). Considering a thickness of about 2,500 m for the Devonian and Carboniferous sedimentary units and about 2,100 m for the missing part of the Vendian and Upper Riphean sedimentary units (Fig. 2), a total of 8,500 m might have overlain the middle part of the Lower Riphean Yusha formation in the Ala-Tau anticlinorium at the end of the Carboniferous. Such a thick sedimentary sequence would lead to a palaeo-temperature gradient of about 23 °C/km at the end of the Carboniferous or Early Permian. This thermal gradient is in accordance with those revealed by apatite fission-track data of Glasmacher et al. (2002) in the Ala-Tau region at the AC-TS'96 transect. Therefore, we suggest that the finite metamorphic grade of the shales in the central and eastern Ala-Tau anticlinorium was reached during Late Carboniferous to Early Permian times.

Inzer synclinorium

In the central part of the AC-TS'96 and URSEIS'95 transects (Ala-Tau to Yamantau Anticlinorium), the significant rapid increase of the diagenetic and incipient metamorphic grades is related to the Zilmerdak thrust and the main Avzyan thrust (Fig. 10). Upper Riphean shales in

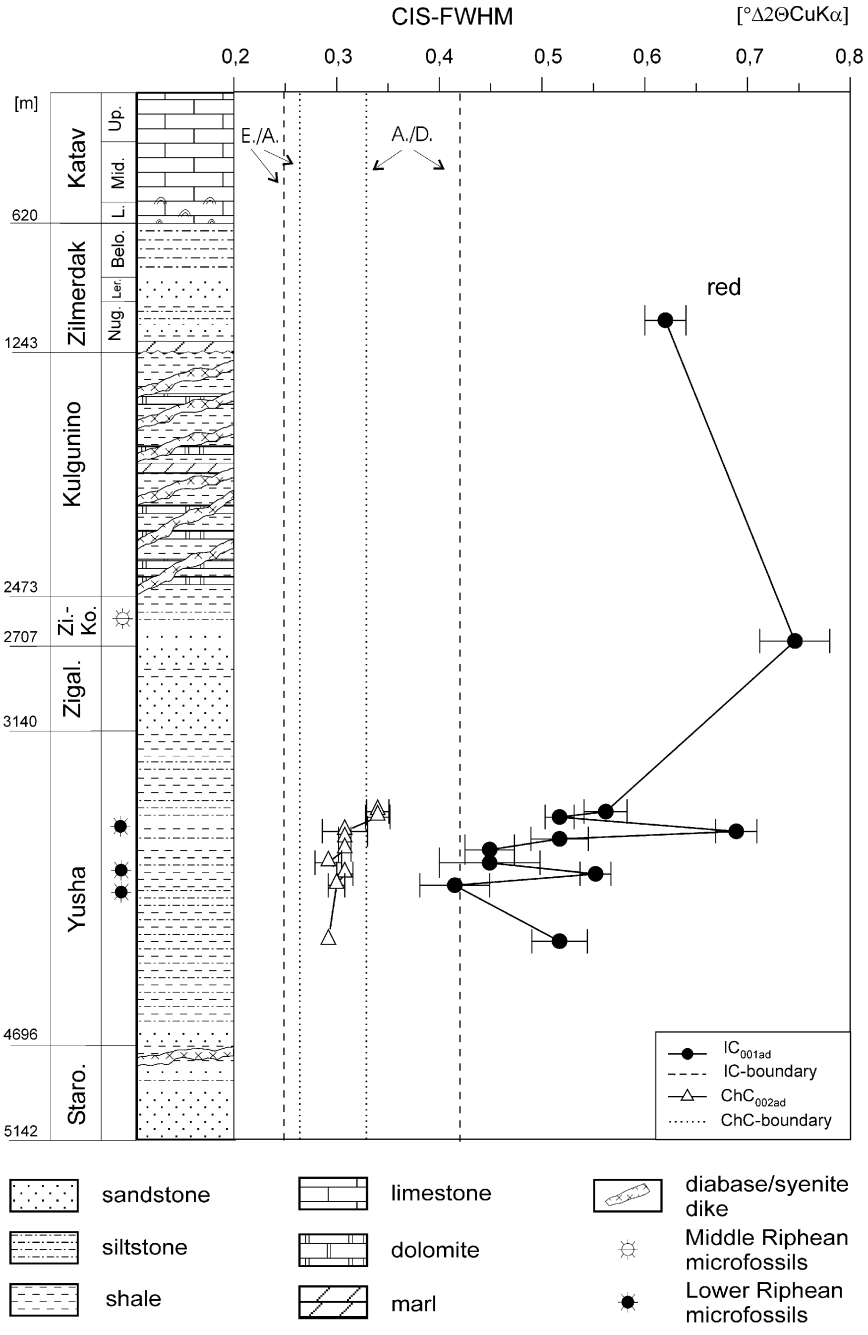

Fig. 9 Comparison of Kübler and Árkai indices from Kul 1 drill hole north of Kulgunino. *D* diagenesis; *A* anchizone; *E* epizone; *red* the only red shale. The upper part of the drillcore between 0 to 1,243 m is characterized by Upper Riphean stromatolitic limestones (0–620 m, Katav) and an intercalation of shales, silt-, and sandstones of Zilmerdak age (620–1,243 m, #DHK-1). The middle section (1,243–2,473 m) consists of a Middle Riphean (Kulgunino) intercalation of shales, marls and dolomites that is crossed by several basaltic and syenitic dikes of various thicknesses. The third section (Middle Riphean) that extends down to the end of the drill hole (5,142 m) is dominated by a 1,556-m-thick sequence (Yusha, 3,140–4,696 m) of black shales and minor dark siltstones (DHK-3–DHK-11). This section is over- and underlain by an intercalation of sandstones with black shales and siltstones (DHK-2). Basaltic dikes also cross the lower part of this section

the footwall of the Zilmerdak thrust (western Inzer synclinorium) show an early diagenesis grade, whereas in the hanging wall, slates of the same stratigraphic age are characterized by a late diagenesis grade. Similarly, at the main Avzyan thrust (eastern Yamantau anticlinorium), slates and phyllites of the same stratigraphic age are of anchizonal grade in the footwall and epizonal (lower greenschist) grade in the hanging wall. Therefore, the age of the metamorphic grade must be older than thrusting. In the Inzer synclinorium, the Kübler index of Middle Riphean slates consistently increases (late diagenesis to middle anchizone) into stratigraphically older rocks. According to Merriman and Frey (1999), the anchizone covers the temperatures between about 200 and 300 °C. The incipient metamorphic grade cannot be explained solely by the thickness (2,500 m, Puchkov 2000) of overlaying Devonian to Carboniferous sediments. If assumed that prior to the deposition of the Palaeozoic sediments, the Precambrian strata were not eroded, about 7,500 m of Upper Riphean and Vendian sedimentary rocks have to be considered. The total amount of about 10,000 m would lead to a palaeo-temperature gradient of about 25 °C/km in Late Carboniferous to Early Permian times, which would be in accordance with a similar palaeo-temperature gradient in the Ala-Tau anticlinorium. Fission-track data of zircon from Middle Riphean sandstone close to the first

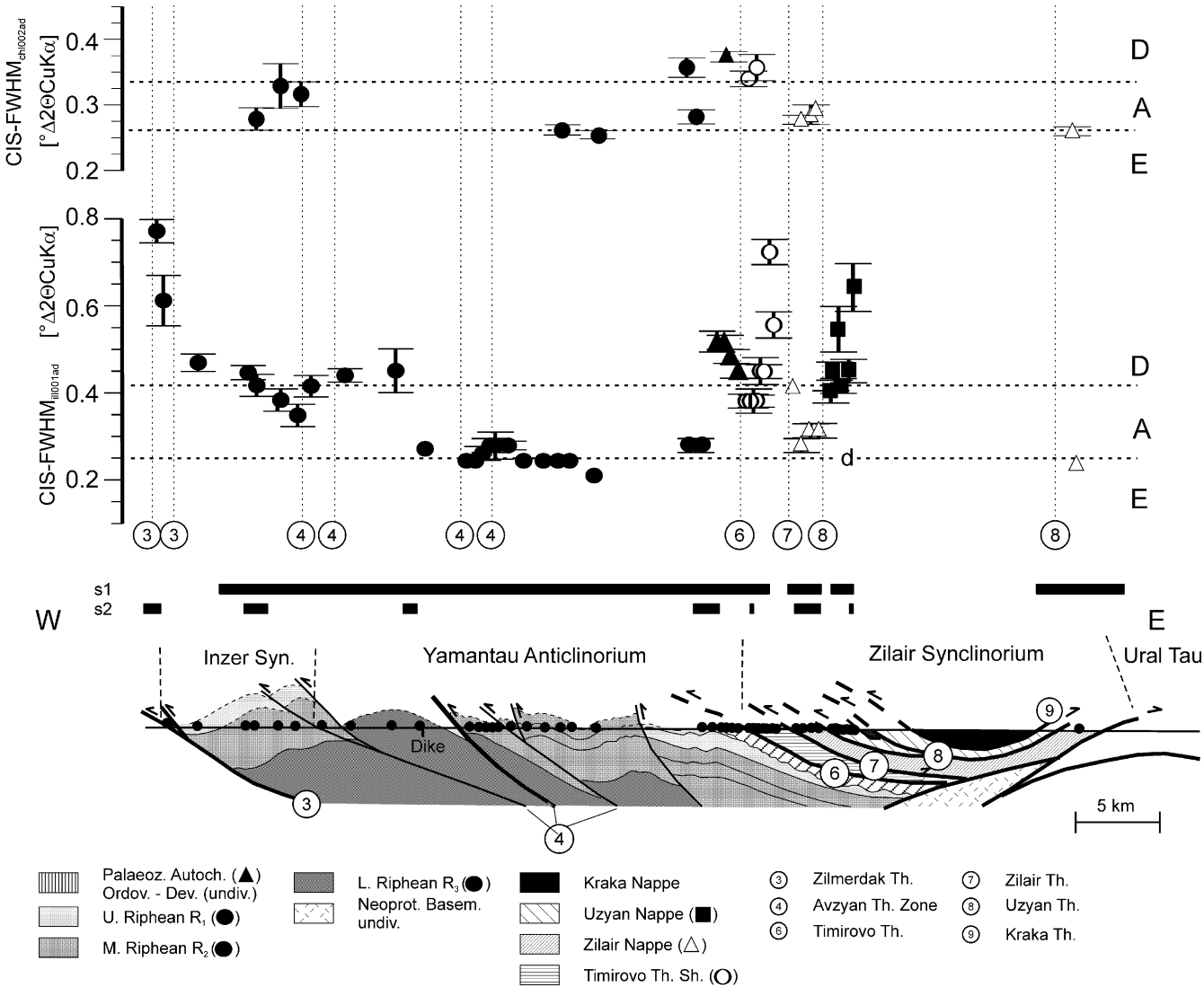

Fig. 10 Comparison of Kübler and Árkai indices from the Ala-Tau anticlinorium, the Inzer synclinorium, the Yamantau anticlinorium and the Zilair synclinorium. *D* diagenesis; *A* anchizone; *E* epizone; *s1* first cleavage; *s2* second cleavage; *d* detrital

Avzyan thrust in the eastern Inzer Synclinorium indicate an age of 604 (100) Ma (Fig. 3; Seward et al. 1997). Kübler index values of surrounding Middle Riphean slates indicate a middle anchizonal grade. As discussed earlier, a temperature of the middle anchizone at geological time scale (~10^6–10^7 years) can partially anneal fission tracks in zircon. Complete annealing of fission-tracks in zircon would need temperatures above 320 °C (Tagami and Shimada 1996; Tagami et al. 1998; Rahn 2001; Brix et al. 2002). Depending on the original detrital age, which must be older than 1,000 Ma, the anchizonal condition could have been reached in Late Carboniferous to Early Permian time.

Yamantau anticlinorium

Lower Riphean slates in the western part of the Yamantau anticlinorium (between the first and third thrust of the Avzyan thrust zone) are characterized by a metamorphic grade at the diagenesis/anchizonal boundary (~200 °C). If the incipient metamorphic grade was reached in Late Carboniferous or Early Permian times, a total thickness of about 16,000 m of Middle Riphean to Late Carboniferous sedimentary rocks have to be considered and would lead to an exceptional low Late Carboniferous or Early Permian palaeo-temperature gradient of about 12 °C/km. Assuming a similar Late Carboniferous or Early Permian palaeo-temperature gradient as the one in the Inzer synclinorium (~25 °C/km), the total thickness would be about 8,000 m. Considering a similar thickness for the Devonian and Carboniferous sedimentary rocks of 2,500 m (Puchkov 2000), about 5,500 m of sedimentary rocks would be of Middle Riphean to Vendian age. The missing thickness of the Middle Riphean to Vendian strata could have been eroded during Lower Palaeozoic denudation that followed the Neoproterozoic orogeny. Nevertheless, it cannot be excluded that the Vendian strata were never deposited in

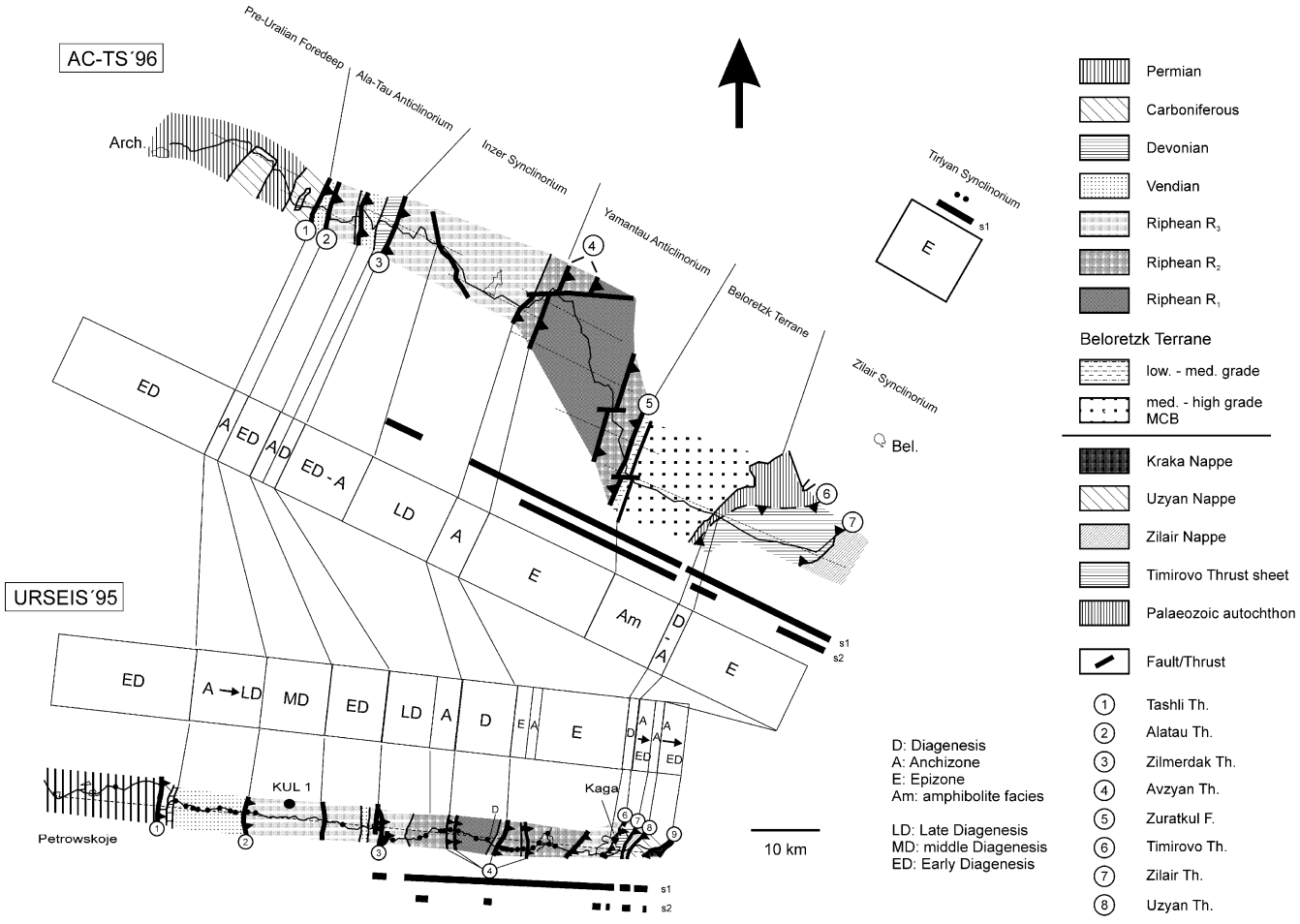

Fig. 11 Comparison of the thermal grade along the AC-TS'96 and the URSEIS'95 transect (based on 1:50,000 scale geological maps). In addition, the distribution of the first (s1) and second (s2) cleavage is displayed

the western part of the Yamantau anticlinorium and that the denudation already started in Vendian time.

In the hanging wall of the third thrust of the Avzyan thrust zone, the Kübler index values of Middle Riphean black slates indicate metamorphic conditions above the epizonal boundary. A zircon fission-track age of 288 (42) Ma from Middle Riphean sandstone indicates movement along the Avzyan thrust in the Early Permian (Seward et al. 1997; Fig. 3). Prior to the Early Permian, the Middle Riphean units must have been at a temperature of more than 320 °C, which is in accordance with the lower greenschist facies metamorphic grade of the Middle Riphean black slates. Green et al. (1996), Tagami et al. (1998), Rahn (2001) and Brix et al. (2002) stated that, for natural zircon samples from various environments, total annealing would be achieved in a reasonable time above about 320 °C. In all geological cases, the duration of the thermal event was in the range of 1–10 Ma. Similarly, as in the western part of the Yamantau anticlinorium, it cannot be excluded that the lower greenschist metamorphic grade was reached in Precambrian time, whereas the final exhumation below about 200 °C occurred in Permian time.

Autochthonous Palaeozoic units and stack of Palaeozoic nappes

Stacking of Palaeozoic siliciclastic and carbonate units along the eastern margin of the BMA, caused by WNW-directed folding and thrusting during the Uralian orogeny (Brown et al. 1996, 1998; Bastida et al. 1997; Puchkov 1997), leads to strong variations of the finite metamorphic grade in shales and slates of the autochthonous Palaeozoic units, the par-autochthonous thrust sheet and the various nappes. The improvement of Kübler index from lower late to upper late diagenetic values in Silurian shales and slates of the autochthonous Palaeozoic units (footwall of E-dipping Timirovo thrust) is W–E directed. In addition, the degree of cleavage increases towards the Timirovo thrust. Therefore, it is very likely that the improvement is partly caused by tectonic strain and not solely related to temperature. Bons (1988) noted that muscovite rarely shows evidence of intracrystalline slip (polygonization) and appears to deform by plastic and elastic processes causing rapid defect migration and crystal growth. Similarly, Merriman et al. (1995) found that white mica rarely shows strain microtextures and appears to have a greater capacity than chlorite to store strain energy, enabling it to

recover from subgrain development by grain boundary migration, i.e. dislocation creep. As a consequence, white mica developed thicker crystallites than chlorite in response to variable strain rates. Furthermore, a relationship between metamorphic grade and tectonic strain was previously described by various authors (Nyk 1985; Roberts and Merriman 1985; Fernández-Caliani and Galán 1992). Within the Timirovo thrust sheet, the metamorphic grade decreases from lower anchizone to lower late diagenesis with stratigraphic age (Lower Silurian to Lower Devonian) and, therefore, might have been developed prior to the emplacement of the nappes. The upper anchizonal metamorphic grade of the Upper Devonian slates of the Zilair nappe is related to the occurrence of two cleavage planes and might be related to the deformation process during nappe emplacement and not solely to temperature.

Conclusion

The Kübler and Árkai indices, as well as earlier published vitrinite reflectance and conodont alteration values (Matenaar et al. 1999), in the western fold-and-thrust belt of the southern Uralides, record various degrees of thermal evolution of the crustal segments prior to the Upper Permo/Triassic and Neoproterozoic orogeny. In the Ala-Tau anticlinorium, the Inzer synclinorium and the western Yamantau anticlinorium, the palaeo-thermal gradient was about 23 to 25 °C in the Late Carboniferous or Early Permian. The increase of diagenetic and incipient metamorphic grade in the hanging wall of all major thrusts indicates a pre-Upper Permo/Triassic deformational origin of nearly all grades. The diagenetic to incipient metamorphic grade displayed in the stack of nappes is mainly related to the emplacement deformation during the Lower Carboniferous.

Pre-Uralian foredeep

Shales of the Pre-Uralian foredeep are characterized by lower, late diagenetic grades. However, apatite fission-track data indicate that the diagenetic grade averages a grade of detrital grains and a grade of in situ formed grains.

Ala-Tau anticlinorium

The incipient metamorphic grade in the western part of the Ala-Tau anticlinorium decreases from the Tashli thrust (middle anchizone) towards the Alatau thrust (diagenesis), and increases from the AC-TS'96 transect in the north to the URSEIS'95 transect in the south. Whereas in the north a palaeo-temperature gradient of about 27 °C/km can account for the incipient metamorphic grade around the Tashli thrust, a palaeo-temperature gradient of more than 30 °C/km is necessary to reach the anchizonal grade in the south. Fission-track data of apatite and zircon indicate that the finite metamorphic grade was reached in Upper Palaeozoic or Permian time.

In the central and eastern part of the Ala-Tau anticlinorium, Upper Riphean sediments are characterized by a lower late to upper late diagenetic grade. The increase of finite metamorphic grade with depth in the Kul 1 drill hole at the URSEIS'95 transect reached diagenesis/anchizonal boundary conditions for the Lower Riphean Yusha formation. The inferred palaeo-temperature gradient of about 23 °C/km at the end of the Carboniferous or Early Permian is in accordance with those revealed by apatite fission-track data in the Ala-Tau region at the AC-TS'96 transect. Therefore, it is very likely that the diagenetic grade in the central and eastern Ala-Tau anticlinorium was reached during Late Carboniferous to Early Permian time.

Inzer synclinorium

In the Inzer synclinorium, the metamorphic grade consistently increases (late diagenesis to middle anchizone) into stratigraphically older rocks. A zircon fission-track age supports middle anchizonal conditions for the Upper Riphean units. A total amount of about 10,000 m of Upper Riphean to Late Carboniferous sedimentary rocks would lead to a palaeo-temperature gradient of about 25 °C/km in Late Carboniferous or Early Permian.

Yamantau anticlinorium

The incipient metamorphic grade in the western part of the Yamantau anticlinorium does not exceed the diagenesis/anchizonal boundary. If the metamorphic grade was reached in the Late Carboniferous or Early Permian, an exceptional low palaeo-temperature gradient of about 12 °C/km would be necessary. Assuming a Late Carboniferous or Early Permian palaeo-temperature gradient of ~25 °C/km, the related total thickness would indicate an Upper Vendian and/or Lower Palaeozoic denudation history that followed the Neoproterozoic orogeny.

In the eastern part of the Yamantau anticlinorium, the metamorphic grade is nearly constant in the epizone. Based on a zircon fission-track age this part of the Yamantau anticlinorium was exhumed along the main Avzyan thrust below about 200 °C in the Early Permian. Similarly as in the western part of the Yamantau anticlinorium it cannot be excluded that the highest metamorphic grade was reached in Precambrian time.

Palaeozoic autochthonous and stack of Palaeozoic nappes

The diagenetic grade increases toward the stack of Palaeozoic nappes. It cannot be excluded that the increase of diagenetic grade is partly caused by deformational process due to the emplacement of the Palaeozoic nappes. Stacking of Palaeozoic siliciclastic and carbonate units along

the eastern margin of the BMA, caused by WNW-directed folding and thrusting during the Uralian orogeny, leads to strong variations of the finite metamorphic grade. Within the Timirovo thrust sheet, the decrease of metamorphic grade with stratigraphic age might have been developed prior to the emplacement of the nappes. The upper anchizonal metamorphic grade of the Upper Devonian slates of the Zilair nappe are related to the occurrence of two cleavage planes and, therefore, is partly caused by the deformation process during nappe emplacement and not solely to temperature.

Acknowledgement The authors like to thank the Deutsche Forschungsgemeinschaft who supported this study with a research grant to the first author. This paper is a contribution to EUROPROBE (URALIDES). EUROPROBE is coordinated within the International Lithosphere Programme and sponsored by the European Science Foundation. We appreciate the critical reading and helpful comments of Dr. Ramseyer, Dr. Barbey and an anonymous reviewer. As a representative for the Russian team during our field work, we thank Dr. V.N. Baryshev and Dr. E. Gorozhanina for their scientific and logistic help.

References

Alekseyev AA (1984) Riphean and Vendian magmatism in the southern Urals (in Russian). Nauka, Moscow

Árkai P (1991) Chlorite crystallinity: an empirical approach and correlation with illite crystallinity, coal rank and mineral facies as exemplified by Palaeozoic and Mesozoic rocks of north-east Hungary. J Metamorph Geol 9:723–734

Árkai P, Sassi FP, Sassi R (1995) Simultaneous measurements of chlorite and illite crystallinity: a more reliable tool for monitoring low- to very low grade metamorphism in metapelites. A case study from the Southern Alps (NE Italy). Eur J Mineral 7:1115–1128

Árkai P, Merriman RJ, Roberts B, Peacor DR, Tóth M (1996) Crystallinity, crystallite size and lattice strain of illite-muscovite and chlorite: comparison of XRD and TEM data for diagenetic and epizonal pelites. Eur J Mineral 8:1119–1137

Árkai P, Balogh K, Frey M (1997) The effects of tectonic strain on crystallinity, apparent mean crystallite size and lattice strain of phyllosilicates in low-temperature metamorphic rocks. A case study from the Glarus overthrust, Switzerland. Schweiz Mineral Petrograph Mitteil 77:27–40

Árkai P, Ferreiro Mählmann R, Suchý V, Balogh K, Sýkorová J, Frey M (2002) Possible effects of tectonic shear strain on phyllosilicates: a case study from the Kandersteg area, Helvetic domain, Central Alps, Switzerland. Schweiz Mineral Petrograph Mitteil 82:273–291

Bastida F, Aller J, Puchkov VN, Juhlin C, Oslianski A (1997) A cross-section through the Zilair Nappe (southern Urals). Tectonophysics 276:253–264

Beane RJ, Connelly JN (2000) $^{40}Ar/^{39}Ar$, U–Pb, and Sm–Nd constraints on the timing of metamorphic events in the Maksyutov Complex, southern Ural Mountains. J Geol Soc Lond 157:811–822

Berzin R, Oncken O, Knapp JH, Pérez-Estaún A, Hismatulin T, Yunusov N, Lipilin A (1996) Orogenic evolution of the Ural Mountains: results from an Integrated seismic experiment. Science 274:10:220–221

Bons A-J (1988) Intracrystalline deformation and slaty cleavage development in very low-grade slates from the Central Pyrénées. Geol Ultraiectina 56:1–173

Brix MR, Stöckhert B, Seidel E, Theye T, Thomson SN, Küster M (2002) Thermobarometric data from a fossil zircon partial annealing zone in high pressure-low temperature rocks of eastern and central Crete, Greece. Tectonophysics 349:309–326

Brown D, Spadea P (1999) Processes of forearc and accretionary complex formation during arc-continent collision in the southern Urals. Geology 27:649–652

Brown D, Puchkov V, Alvarez-Marron J, Perez-Estaun A (1996) The structural architecture of the footwall to the Main Uralian Fault, southern Urals. Earth Sci Rev 40:125–147

Brown D, Alvarez-Marron J, Perez-Estaun A, Gorozhanina Y, Baryshev V, Puchkov V (1997) Geometric and kinematic evolution of the foreland thrust and fold belt in the southern Urals. Tectonics 16:551–562

Brown D, Juhlin C, Alvarez-Marron J, Perez-Estaun A, Oslianski A (1998) Crustal-scale structure and evolution of an arc-continent collision zone in the southern Urals, Russia. Tectonics 17:158–171

Brown D, Alvarez-Marron J, Perez-Estaun A, Puchkov V, Ayala C (1999) Basement influence on foreland thrust and fold belt development: an example from the southern Urals. Tectonophysics 308:459–472

Brown D, Hetzel R, Scarrow JH (2000) Tracking the arc-continent collision subduction zone processes from high-pressure rocks in the southern Urals. J Geol Soc Lond 157:901–904

Brown D, Alvarez-Marron J, Perez-Estaun A, Puchkov V, Ayarza P, Gorozhanina Y (2001) Structure and evolution of the Magnitogorsk forearc basin: Identifying upper crustal processes during arc-continent collision in the southern Urals. Tectonics 20:364–375

Döring J, Götze HJ (1999) The isostatic state of the southern Urals crust. Geol Rundsch 87:500–510

Echtler HP, Hetzel R (1997) Main Uralian thrust and main Uralian normal fault: non-extensional Palaeozoic high-P rock exhumation, oblique collision and normal faulting in the southern Urals. Terra Nova 9:158–162

Echtler HP, Stiller M, Steinhoff F, Krawczyk C, Suleimanov V, Knapp JH, Menshikov Y, Alvarez-Marrón J, Yunusov N (1996) Preserved collisional crustal structure of the southern Urals revealed by Vibroseis profiling. Science 274:224–226

Fernández-Caliani J, Galan E (1992) Influence of tectonic factors on illite crystallinity: a case study in the Iberian Pyrite Belt. Clay Miner 27:385–388

Frank B (1987) Bestimmung des Metamorphosegrades der paläozoischen Schichten des Venn-Großsattels (Linksrheinisches Schiefergebirge) mit Hilfe der Illit-Kristallinität und Untersuchung der Zusammenhänge zwischen dem metamorphosegrad und den regionalen tektonischen Verhältnissen. Doktorarbeit RWTH Aachen

Giese U (2000) The western fold-and-thrust-belt of the southern Urals, Russia: review and perspective. N Jb Geol Paläont Abh 218:267–284

Giese U, Glasmacher UA, Kozlov V, Matenaar I, Puchkov V, Stroink L, Bauer W, Ladage S, Walter R (1999) Structural framework of the Bashkirian Anticlinorium, SW Urals. Geol Rundsch 87:526–544

Glasmacher U, Matenaar I, Pickel W, Giese U, Kozlov VI, Puchkov V, Stroink L, Walter R (1997) Incipient metamorphism of the western fold-and-thrust belt, southern Urals, Russia. Beih Eur J Mineral 9:124

Glasmacher UA, Reynolds P, Alekseev A, Puchkov V, Taylor K, Gorozhanin V, Walter R (1999) $^{40}Ar/^{39}Ar$ Thermochronology west of the Main Uralian Fault, southern Urals, Russia. Geol Rundsch 87:515–525

Glasmacher UA, Bauer W, Giese U, Reynolds P, Kober B, Puchkov VN, Stroink L, Alekseev A, Willner A (2001) The metamorphic complex of Beloretzk, SW Urals, Russia: a terrane with a polyphase Meso- to Neoproterozoic thermo-dynamic evolution. Precambrian Res 110:185–213

Glasmacher UA, Wagner GA, Puchkov VN (2002) Thermo-tectonic evolution of the western Fold-and-Thrust belt, southern Urals, Russia, as revealed by apatite fission-track data. Tectonophysics 354:25–48

Glodny J, Bingen B, Austrheim H, Molina JF, Rusin A (2002) Precise eclogitization ages deduced from Rb/Sr mineral systematics: the Maksyutov complex, southern Urals, Russia. Geochim Cosmochim Acta 66:1221–1235

Graver JI, Bartholomew A (2001) Partial resetting of fission tracks in detrital zircon: dating low temperature events in the Hudson Valley (NY). Geophys Soc Am Abstr Programs 33:83

Green PF, Hegarty KA, Duddy IR, Foland SS, Gorbachev V (1996) Geological constraints on fission track annealing in zircon. Abstract of presentation at the Int. Workshop on Fission Track Dating, Gent

Guggenheim S, Bain DC, Bergaya F, Brigatti MF, Drits VA, Eberl DD, Formoso MLL, Galán E, Merriman RJ, Peacor DR, Stanjek H, Watanabe T (2002) Report of the association internationale pour L'Étude des argyles (AIPEA) nomenclature committee for 2001: order, disorder and crystallinity in phyllosilicates and the use of the "Crystallinity index". Clays Clay Minerals 50:406–409

Hamilton W (1970) The Uralides and the motion of the Russian and Siberian platforms. Geol Soc Am Bull 81:2553–2576

Haq BU, Eysinga van FWB (1998) Geological time table, 5th edn. Elsevier Science, Amsterdam

Harrison TM, Armstrong RL, Naeser CW, Harakal JE (1979) Geochronology and thermal history of the Coast Plutonic Complex, near Prince Rupert, British Columbia. Can J Earth Sci 16:400–410

Hasebe N, Mori S, Tagami T, Matsui R (2003) Geological partial annealing zone of zircon fission-track system: additional constrains from the deep drilling MITI-Nishikubiki and MITI-Mishima. Chem Geol 199:45–52

Hetzel R, Echtler HP, Seifert W, Schulte BA, Ivanov KS (1998) Subduction- and exhumation-related fabrics in the Palaeozoic high-pressure/low-temperature Maksyutov Complex, Antingan area, southern Urals, Russia. Bull Geol Soc Am 110:916–930

Jacob G, Kisch HJ, Pluijm van der BA (2000) The relationship of phyllosilicate orientation, X-ray diffraction intensity ratios, and c/b fissility ratios in metasedimentary rocks of the Helvetic zone of the Swiss Alps and the Caledonides of Jämland, central western Sweden. J Struct Geol 22:245–258

Kasuya HG, Naeser CW (1988) The effect of α-damage of fission-track annealing in zircon. Nucl Tracks Radiat Measure 14:477–480

Kisch HJ (1991) Illite crystallinity: recommendations on sample preparation, X-ray diffraction settings, and interlaboratory samples. J Metamorph Geol 9:665–670

Kozlov VI (1982) Upper Riphean and Vendian in the South Urals (in Russian). Nauka, Moscow

Kozlov VI, Krasnobaev AA, Larionov NN, Maslov AV, Sergeeva ND, Ronkin YuL, Bibikova EV (1989) Lower Riphean of the south Urals (in Russian). Nauka, Moscow

Kozlov VI, Sinitsyna ZA, Kulagina EI, Pazukhin VN, Puchkov VN, Kochetkova NM, Abramova AN, Klimenko TV, Sergeeeva ND (1995) Guidebook of excursion for the Palaeozoic and Upper Precambrian sections of the Western slope of the southern Urals and Preuralian regions. Geol Inst Ufa Sci Center RASci, Ufa

Krumm S, Buggisch W (1991) Sample preparation effects on illite crystallinity measurement: grain-size gradation and particle orientation. J Metamorph Geol 9:671–677

Leech ML (2001) Arrested orogenic development: eclogitization, delamination, and tectonic collapse. Earth Planet Sci Lett 185: 149–159

Maslov AV, Erdtmann BD, Ivanov KS, Ivanov SN, Krupenin MT (1997) The main tectonic events, depositional history, and the paleogeography of the southern Urals during the Riphean–Early Palaeozoic. Tectonophysics 276(1–4):313–335

Matenaar I, Glasmacher UA, Pickel W, Giese U, Pazukhin VN, Kozlov VI, Puchkov VN, Stroink L, Walter R (1999) Incipient metamorphism between Ufa and Beloretzk, western fold-and-thrust belt, southern Urals, Russia. Geol Rundsch 87:545–560

Matte P, Maluski H, Caby R, Nicolas A, Kepezhinskas P, Sobolev S (1993) Geodynamic model and $^{39}Ar/^{40}Ar$ dating for the generation and emplacement of the high pressure (HP) metamorphic rocks in SW Urals. CR Acad Sci Ser II, 317:1667–1674

Merriman RJ, Frey M (1999) Patterns of very low-grade metamorphism in metapelitic rocks. In: Frey M, Robinson D (eds) Low-grade metamorphism. Blackwell Science, Oxford, pp 61–107

Merriman RJ, Peacor DR (1999) Very low-grade metapelites: mineralogy, microfabrics and measuring reaction progress. In: Frey M, Robinson D (eds) Low-grade metamorphism. Blackwell Science, Oxford, pp 10–60

Merriman RJ, Roberts B, Peacor DR, Hirons SR (1995) Strain-related differences in the crystal growth of white mica and chlorite: a TEM and XRD study of the development of metapelites microfabrics in the Southern Uplands thrust terrane, Scotland. J Metamorph Geol 13:559–576

Nierhoff R (1994) Metamorphose-Entwicklung im Linksrheinischen Schiefergebirge: Metamorphosegrad und -verteilung sowie Metamorphosealter nach K–Ar-Datierungen. Aachener Geowiss. Beitr. 3, Aachen

Nyk R (1985) Illite crystallinity in Devonian slates of the Meggen mine (Rhenish Massif). N Jb Miner Mh 268–276

Passchier CW, Trouw RAJ (1996) Microtectonics. Springer, Berlin Heidelberg New York

Puchkov VN (1988) Pre-Alpine tectonic features throughout and around the Alpine orogen. Acta Geol Palonica XXI:45–65

Puchkov VN (1993) The paleo-oceanic structures of the Ural Mountains. Geotectonics 27:184–196

Puchkov VN (1997) Structure and geodynamics of the Uralian orogen. In: Burg JP, Ford M (eds) Orogeny through time. Geol Soc Lond Spec Publ 121:201–236

Puchkov VN (2000) Palaeogeodynamics of the central and southern Urals. Ufa, Pauria

Rahn MKW (2001) The metamorphic and exhumation history of the Helvetic Alps, Switzerland, as revealed by apatite and zircon fission tracks. Habilitation Thesis, Universität Freiburg

Remaine J, Cita MB, Dercourt J (2000) International Stratigraphic Chart and Explanatory Note, IUGS-UNESCO

Reuter A (1985) Korngrößenabhängigkeit von K–Ar-Datierungen und Illit-Kristallinität anchizonaler Metapelite und assoziierter Metatuffe aus dem östlichen Rheinischen Schiefergebirge. Göttinger Arb Geol Paläont 27:1–91

Riley BCD (2002) Preferential thermal resetting of fission tracks in radiation-damaged detrital zircon grains: case study from the Laramide of Arizona. Geophys Soc Am Abstr Programs 34:paper no 212-12

Roberts B, Merriman RJ (1985) The distinction between Caledonian burial and regional metamorphism in metapelites from North Wales: an analysis of isocryst patterns. J Geol Soc 142:615–624

Semikhatov MA, Shurkin KA, Aksenov EM et al. (1991) A new Precambrian stratigraphic scale in the USSR. Isv AN USSR Ser Geol 4:3-13

Seward D, Pérez-Estaún A, Puchkov VN (1997) Preliminary fission-track results from the southern Urals: Sterlitamak to Magnitogorsk. Tectonophysics 276:281–290

Shatsky VS, Jagoutz E, Koz'menko OA (1997) Sm–Nd dating of the high-pressure metamorphism of the Maksyutov Complex, southern Urals, Dokl (English translation). Akad Sci USSR, Earth Sci Ser 353:285–288

Steer DN, Knapp JH, Brown LD, Echtler HP, Brown DL, Berzin R (1998) Deep structure of the continental lithosphere in an unextended orogen: an explosive-source seismic reflection profile in the Urals (Urals Seismic Experiment and Integrated Studies URS-EIS 1995). Tectonics 17:143–157

Stroink L, Frese K, Giese U, Matenaar I, Kozlov VI, Glasmacher U, Puchkov V, Walter R (1997) Compositional framework of Upper Proterozoic sandstones of the southern Urals: implications for a Pre-Uralian orogenic event. 18th IAS, Heidelberg, GAEA 3:324

Tagami T, Shimada C (1996) Natural long-term annealing of zircon fission track system around a granitic pluton. J Geophys Res B 101:11353–11364

Tagami T, Galbraith RF, Yamanda R, Laslett GM (1998) Revised annealing kinetics of fission tracks in zircon and geological implications. In: Van den haute P, De Corte F (eds) Advances in fission-track geochronology. Kluwer, Dordrecht, pp 99–112

Tschernoster R (1995) K–Ar-Datierungen von Mikneralphasen ausgewählter Metamagmatite und Metapelite aus dem Stavelot-Venn-Massiv. Diplomarbeit RWTH Aachen

Wang H, Frey M, Stern WB (1996) Diagenesis and metamorphism of clay minerals in the Helvetic Alps of Eastern Switzerland. Clays Clay Minerals 44:96–112

Warr LN, Rice AHN (1994) Interlaboratory standardization and calibration of clay mineral crystallinity and crystallite size data. J Metamorph Geol 12:141–152

Willner AP, Emolaeva T, Stroink L, Glasmacher UA, Giese U, Puchkov V, Kozlov VI, Walter R (2001) Contrasting provenance signals in Riphean and Vendian sandstones in the SW Urals (Russia): constraints for a change from passive to active continental margin conditions in the Neoproterozoic. Precambrian Res 110:215–239

Yamada R, Tagami T, Nishimura S, Ito H (1995) Annealing kinetics of fission tracks in zircon: an experimental study. Chem Geol 122:249–258

Zonenshain LP, Korinevsky VG, Kazmin VG, Pechersky DM, Khain VV, Mateveenkov VV (1984) Plate tectonic model of the south Urals development. Tectonophysics 109:95–135

Zonenshain LP, Kuzmin MI, Natapov LM (1990) Uralian Foldbelt. In: Page BM (ed) Geology of the USSR: a plate-tectonic synthesis. Geodyn Ser, vol 21. Am Geophys Union, Washington, DC, pp 27–54